E. McGlynn, M.O. Henry, and J.-P. Mosnier

School of Physical Sciences / National Centre for Plasma Science & Technology
Dublin City University, Dublin, Ireland

ZNO WIDE BANDGAP SEMICONDUCTOR NANOSTRUCTURES: GROWTH, CHARACTERIZATION AND APPLICATIONS

E.McGlynn, M.O. Henry and J.-P. Mosnier

1. INTRODUCTION

The compound ZnO, or zincite, has a long, fascinating and diverse history displaying a number of peaks and troughs in terms of the degree of research interest, numbers of publications per annum and so forth. These peaks have in some cases been associated with the discovery of a new aspect of its behaviour which is relevant to some scientific or technological focus (such as UV light emission) and the ambitions associated with these technologies. Some of these ambitions have been realized and some, to date, remain ambitions. The general public will most probably know of this material from some of its earlier applications. Zinc oxide was initially known by a variety of names, some of rather unclear origin, including “nihil album”, “flowers of zinc”, “chinese white” and “philosopher’s wool”. The usage of these terms has obviously declined since the standardization of chemical nomenclature since the early 1800’s as discussed by Kent (1958). ZnO is, or has been, used as a pigment in paints and enamel coatings (hence the name “chinese white”) and also as an ingredient in cements, glass, tires, glue, matches, white ink, reagents, photocopy paper, flame retardant, fungicides, cosmetics and dental cements and ~ 100,000 tonnes of ZnO is produced per annum as reported by Klingshirn (2007). These diverse applications rely on various properties of ZnO such as the white colour of the material, its chemical activity, UV blocking capability, heat conductivity and bioactivity. ZnO is used extensively in various pharmaceutical and cosmetic products including ointments and sunscreen preparations

(including an appearance in the Hollywood movie “Jaws”, where Brody’s wife enquires if he has remembered to bring the zinc oxide sunscreen before he boards the Orca). ZnO is a material which is used in a very wide variety of applications in a diverse range of technological spaces. In addition to this already impressive technological resume, ZnO is used widely in the semiconductor industry, primarily in varistor manufacture, but also as a transparent conducting oxide, a photoconductor and a phosphor, see e.g. Klingshirn (2007), Minami (2005), Monroy et al. (2003) and Heiland et al. (1959).

A graph of the number of records returned by a search on the keywords (ZnO) OR (“zinc oxide”) in ISI Web of Science[SM] is shown in figure 1 (including 2007) and a clear growth in the 1960’s and a plateau thereafter is seen followed by an explosion of activity around 1990 continuing to the present. It appears that the loss of interest in the period 1970 – 1990 was due in part to severe difficulties in doping the material p-type effectively, an issue which remains a severe handicap. It is also likely that the rapid advances associated with the new physics being discovered in III-V low dimensional structures drew many researchers away from this difficult problem. The pattern of discovery and rediscovery has been commented upon explicitly by Prof. Claus Klingshirn (2005, one of a number of investigators who have witnessed both periods of growth in ZnO actvity) in his paper “ZnO rediscovered – once again!?”. This title alluded to a publication by M.E. Brown (1957) titled “ZnO – Rediscovered”. The most recent period of intense activity in ZnO research seems to have grown from a number of converging factors including the publication of a number of papers where optically pumped lasing effects are seen in thin films and nanostructures at room temperature as reported e.g. by Zu et al. (1997) and Bagnall et al. (1998). This was combined with the explosive developments in GaN research, leading to short wavelength LEDs and LDs, and the demonstration of large markets for such devices, which led researchers back to ZnO as a potential competitor to GaN, with significant intrinsic material advantages including the availability of high quality large area substrates suitable for homopeitaxy and the larger exciton binding energy of ZnO, promising efficient excitonic emission at room temperature and higher as discussed by Look (2001).

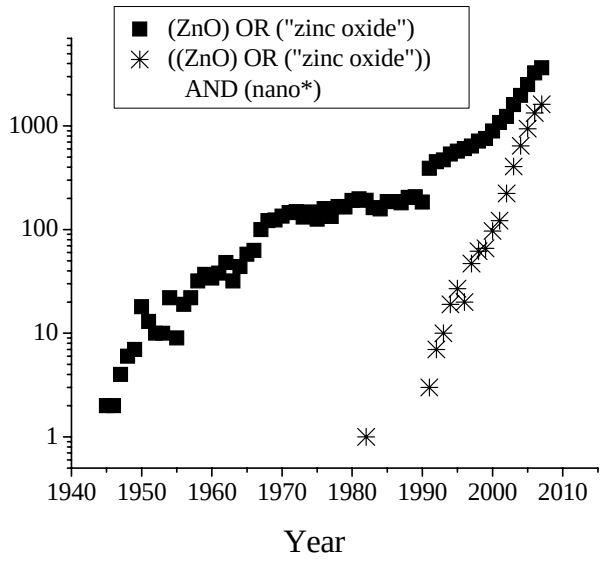

Fig. 1: Records returned by a search on the keywords “*(ZnO) OR (“zinc oxide”)*” or “*((ZnO) OR (“zinc oxide”)) AND (nano*)*” in ISI Web of Science[SM] (conducted on 31st March 2008).

The present period of growth has however brought with it a new aspect to ZnO research. It had been known from the 1940s that ZnO grows in the form of various nanostructures under a variety of growth conditions; see e.g. Klingshirn (2007), Park et al. (1967), Scharowsky (1953) and Fuller (1944). The present era of research using a variety of common thin film growth techniques (in many cases developed and perfected during the 1970's and 1980's for III-V materials) has shown that these needle-like and other nanostructures may often have diameters in the range 50 – 200 nm and thus the new era of ZnO research has been inextricably bound up with the growth, characterization and application of these ZnO nanostructures. Figure 1 also shows the results of a search on the keywords ((ZnO) OR ("zinc oxide")) AND (nano*) in ISI Web of Science. The trend here is clear, with activity beginning around 1990 and growing exponentially from that time to the present. In fact ZnO appears to grow in nanostructured form rather easily, on a variety of substrates, at various temperatures and in many cases shows self-organised behaviour, with e.g. preferential nanorod alignment perpendicular to the substrate; see e.g. Wang (2004). This ease of growth and self-organisation has certainly contributed to the widespread activity in

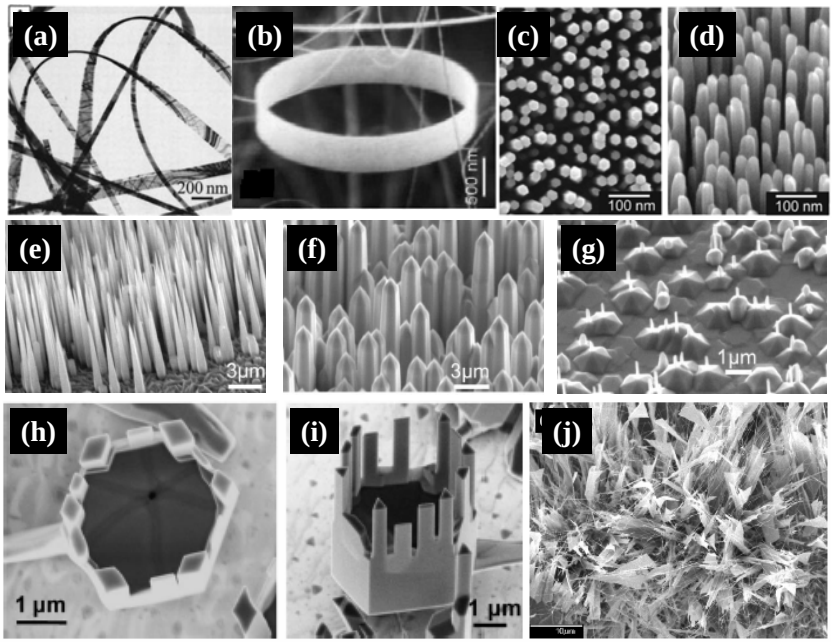

Fig 2: Selection of TEM/SEM images of ZnO nanostructures from the published literature including: (a) nanobelts, (b) nanorings, (c) and (d) nanorod arrays, (e) nanoneedles, (f) hexagonal ZnO nanocrystallites, (g) hexagonal ZnO microdots with wires on top, (h) and (i) nanocastles, (j) nanoflowers. Image (a) from Z.W. Pan, Science, 291, 1947 (2001). Copyright 2001. Reprinted with permission from AAAS. Image (b) from X.Y. Kong, Science, 303, 1348 (2004). Copyright 2004. Reprinted with permission from AAAS. Images (c) and (d) reprinted with permission from W. I. Park, Applied Physics Letters, 80, 4232 (2002). Copyright 2002, American Institute of Physics. Images (e) – (g) reprinted with permission from M. Lorenz, Applied Physics Letters, 86, 143113 (2005). Copyright 2005, American Institute of Physics. Images (h) and (i) reprinted with permission from X.D. Wang, Chemical Physics Letters, 424, 86 (2006). Copyright 2006, Elsevier Publishing. Image (j) reused with permission from F. Xu, Nanotechnology, 17, 2855 (2006). Copyright 2006, Institute of Physics.

this field. A bewildering assortment of diverse nanoscale morphologies has been reported, including ZnO wires, rods, needles, pins, belts and helices; see e.g. Wang (2004), Wang (2008) and Lorenz et al. (2005). In addition such exotic sounding varieties as nanotetrapods, nanoflowers, nanocastles and nanopigtails have also been reported; see e.g. Wang et al. (2006a), Xu et al. (2006) and Ding et al. (2007a). A selection of scanning electron microscopy (SEM) and transmission electron microscopy (TEM) images of such structures reported in the literature is shown in figure 2.

This diversity of achievable morphologies has spurred many researchers forward during the past decade. However, hidden in the diversity we must eventually acknowledge and confront a rather worrying and difficult reality. From the many discussions involving the authors at a variety of international meetings and conferences (including recent EMRS meetings, Photonics West, EU SOXESS meetings and others) it is widely acknowledged in the community that the morphology of ZnO nanostructures is highly sensitive to the growth environment (e.g. parameters such as temperature, pressure, substrate choice and gas flow). The content of these discussions is borne out by our own experience, though the matter is commented upon rather less in published articles in peer-reviewed journals. This sensitivity is the origin of the diversity observed and commented upon above and makes it very difficult to control the growth process to a sufficient degree to achieve large area uniform growth of a particular desired morphology reproducibly. It has generally proven especially difficult to take a published growth recipe from one laboratory and reproduce the results using the same recipe in another laboratory. However, it is also the case that certain growth techniques (such as e.g. metal organic chemical vapour deposition (MOCVD) discussed in section 3.2 below) seem to show a greater degree of reproducibility than others in this respect. Generally however one of the main challenges which ZnO nanostructure research will face in the next 5 years is how to control growth to synthesize desired nanostructure morphologies reproducibly and uniformly over a large area substrate. It is only by meeting this challenge that the technological potential shown to date in the wide morphological diversity of ZnO nanostructures can be transferred to the stage of device manufacture on a commercial scale.

The reasons why this new aspect of ZnO research, ZnO nanostructures, is so important, and exciting such interest, are based around the many new scientific and technological possibilities which such structures offer. At the simplest level, many wide bandgap semiconductors (including ZnO) are very poorly lattice matched to commonly and cost effective substrates such as Si and sapphire. This has severely limited the material quality of ZnO thin films. The small contact area (or “footprint”) of ZnO nanostructures on such substrates means that deleterious strain effects are much reduced, and the sidewalls of the nanostructures can relax to accommodate residual strain. As a result ZnO nanostructures grown by many methods are almost perfect single crystals, and their optical and other properties are exceedingly good; see e.g. Voss et al. (2006). In addition, new properties intrinsically associated with the large surface to volume ratio of such nanomorphologies have emerged. Examples of such developments include studies on the bound surface exciton by Grabowska et al. (2005) in addition to work on sensing, photochemistry and energy production where the surface to volume ratio provides key technical advantages, see e.g. Wang (2007) and Willander et al. (2008a). The nanostructured morphology, sometimes in

combination with other ZnO material properties such as its mechanical robustness, has led to very promising applications in areas such as field emission sources for light-emitting structures and piezo-electric energy production.

It is the aim of this article to introduce the reader to the basic physics and materials science of ZnO (section 2), to outline some of the commonly used growth methods (section 3) and results of characterization of ZnO nanostructures (section 4). Section 5 will conclude the chapter by providing a brief introduction to some promising areas of application of ZnO nanostructures. Referring to figure 1, we note that the number of ZnO related publications reaches almost 22,000 since 1990 (with keywords (ZnO) OR ("zinc oxide")) while the number of ZnO publications related to nanostructures (with keywords ((ZnO) OR ("zinc oxide")) AND (nano*)) reaches almost 6,000 in the same period. Given the vast literature on the subject, it is clear (a) that the choice of topics within the following sections is not exhaustive or even representative of the breadth of the published works and (b) that the references are purely indicative rather than a detailed and comprehensive bibliography of the subject. Thus, in advance, we apologise to both the readers for such partial choices of references and to colleagues in the ZnO field if we have neglected to reference their particular contributions in certain sections.

2. ZNO WIDE BANDGAP SEMICONDUCTORS: CRYSTALLLINE AND ELECTRONIC STRUCTURE AND OPTICAL AND MATERIALS PROPERTIES

2.1 ZnO crystal structure and related topics

At standard temperature and pressure ZnO crystallizes in the hexagonal wurtzite crystal structure, shown in figure 3 The space group for wurtzite crystals is C_{6v}^4 or $P6_3mc$ (#186) and the point group is C_{6v} or 6 mm as reported by Casella (1959). The crystal structure was determined early in the twentieth century by a number of workers including Weber (1923), Bragg (1920) and Bunn (1935) in the period 1923-1935 and further refinements of the lattice constants have been published since that time. The currently accepted values of the lattice constants are $c \approx 0.521$ nm and $a \approx 0.325$ nm (see e.g. powder diffraction file # 36-1451 from the International Centre for Diffraction Data, ICDD). Each atom (either Zn or O) is surrounded by 4 other atoms (O or Zn, respectively) and bonds to them to form a slightly distorted tetrahedral configuration ($c/a_{\text{actual}} = 1.602$ compared to $c/a_{\text{ideal}} = 1.633$ for perfect close packing) and the unit cell contains 4 atoms.

The bonding of Zn and O can be adequately described within the usual scheme of sp^3 hybridisation (to be discussed further in section 2.2 below) used for tetrahedrally coordinated semiconductor compounds but is more ionic than is the case in the III-V compound semiconductors with a value of the Phillip's (1970) ionicity parameter of 0.616, placing it at the border between classification as ionic or covalently bonded.

The tetrahedral bonding gives rise to different polarity characteristics for various crystal surfaces, as defined by Tasker (1979). Specifically, the (0001) and (000-1) basal crystal faces,

are polar faces, Zn- and O-terminated, respectively. The prismatic {11-20} and {10-10} faces are non-polar, while faces such as (11-21) have a mixed polarity character. The presence of polar faces gives rise to a number of properties of interest for ZnO material generally, and for ZnO nanostructures in particular, including spontaneous electrical polarization, piezo-electricity, preferential growth and etching along such directions as discussed by Wang (2004) and (2007).

Because of the presence of 4 atoms in its unit cell, ZnO has 3 acoustic phonon branches (two transverse and one longitudinal) and (3 x 4) – 3 = 9 optical phonon branches. The energies and symmetries of these phonon modes at the Brillouin zone centre are listed in the review by Klingshirn (2007). The phonon energies at the Γ-point range from ~12 meV to 72 meV and have symmetries associated with the Γ_1, Γ_3, Γ_5 and Γ_6 representations of the crystal point group and the Γ_1 and Γ_5 phonon modes are the optically active (dipole allowed) modes showing a longitudinal transverse splitting in both cases of ~ 22 – 24 meV. The optically active LO modes both have energies of ~ 72 meV and interact strongly with quasiparticles such as excitons and LO phonon replica associated with such interactions are observed in both photoluminescence (PL) and resonant Raman scattering (Klingshirn (1975) and Scott (1970)). The Γ_1, Γ_5 and Γ_6 phonon modes are Raman active and the absence of inversion symmetry in the crystal means that some phonon modes are both optically and Raman active; see e.g. Klingshirn (2007) and the references therein.

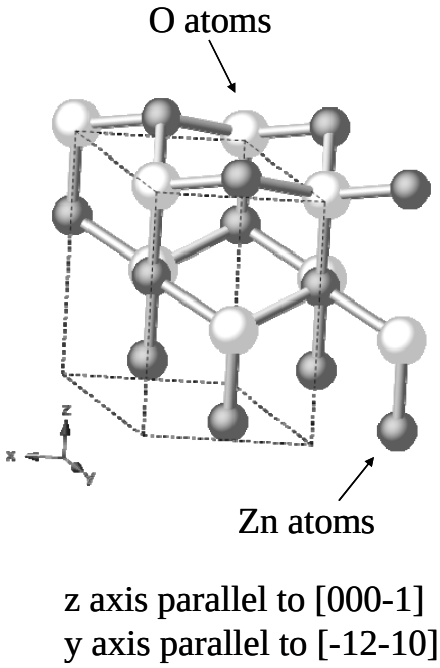

Fig. 3: ZnO hexagonal wurtzite crystal structure, with axes and unit cell shown (images created using CrystalMaker, a crystal and/or molecular structure program.

In addition to the wurtzite (B4) phase, ZnO can also crystallize in the rocksalt (B1 – NaCl) structure at high pressures, and may crystallize in the zinc-blende (B3) structure e.g. when grown on cubic substrates. The ZnO B1 rocksalt structure was reported for applied pressures above 9.5 GPa, and is also known to be metastable at room temperature and atmospheric pressure, reported by Recio et al. (1998) and Bates et al. (1962). The B3 zinc-blende structure has been reported for growth on Pt thin films by Kim et al. (2003a)) and also via growth on GaAs by Almamun Ashrafi et al. (2000). The zinc-blende phase has also been reported recently by Ding et al. (2007a) to play a key role in the nucleation and initial growth stages of ZnO nanotetrapods, similar to tetrapod nanostructures of other II-VI semiconductors such as

CdTe, CdS, ZnS, ZnSe and CdSe, despite the higher stability of the bulk wurtzite phase in ZnO compared to these other materials due to its strong ionic binding.

Relatively recently, some very exciting developments have been reported in theoretical studies of initial thin film growth of ZnO and also in theoretical studies of nanowire stress loading. A long standing controversy has existed over the mechanism by which the common *c*-axis orientation of thin films is stabilized against surface reconstruction due to the divergent surface energy associated with polar surfaces. Theoretical work has predicted that in the initial phases (~ 10 – 20 monolayers) of film growth, ZnO (and wurtzite films generally) may grow with a non-polar graphitic structure which fixes the *c*-axis orientation; see reports by Freeman et al. (2006) and Claeyssens et al. (2005). Further growth then causes a transition to a wurtzite structure with a low or zero energy barrier. Similar theoretical results have been reported for the growth evolution of MgO (111) films also by Goniakowski et al. (2004). These theoretical predictions have recently been substantiated in the case of ZnO by surface x-ray diffraction and scanning tunneling microscopy (STM) by Tusche et al. (2007). First principles calculations also predict that a wurtzite to graphitic transformation should occur in [01-10] oriented nanowires under uniaxial tensile loading of ~ 10 GPa, as reported by Kulkarni et al. (2006). In addition to the long-known B1 and B3 rocksalt and zinc-blende phases, the non-polar graphitic phase may be very important in determining the nucleation and growth of ZnO nanostructures and also aspects of their behaviour under stress, an aspect which is of importance in application areas of ZnO nanostructures such as sensing and piezo-electric energy production.

2.2 ZnO electronic bandstructure

As noted above, the electronic bandstructure of ZnO can be described using the model of sp^3 hybridisation commonly applied to a range of tetrahedrally coordinated semiconductor compounds. ZnO is a direct bandgap material and the ionic nature of the bonding means that the bottom of the conduction band at the Brillouin zone centre is formed predominantly from the Zn^{2+} 4s levels while the top of the valence band at the zone centre is formed from the O^{2-} 2p levels; see Klingshirn (2007). Based on these atomic states and using the compatibility relationships for the C_{6v} group associated with the zone centre, the orbital level of the ZnO conduction band at the zone centre will be a non-degenerate Γ_1 level, while the 3-fold degenerate p states making the valence band will split into a Γ_1 and a Γ_5 level. When the electron spin and the effects of spin orbit coupling are included, using the C_{6v} double group the conduction band becomes a $\Gamma_1 \otimes \Gamma_7 = \Gamma_7$ level, while the valence band splits into $(\Gamma_1 \oplus \Gamma_5) \otimes \Gamma_7 = \Gamma_7 \oplus \Gamma_9 \oplus \Gamma_7$, i.e. three spin degenerate Kramer's doublets. Thus ZnO has three valence bands (named A, B and C in order of increasing energy separation from the conduction band, a convention followed for all wurtzite semiconductors). The band structure at the zone centre is shown schematically in figure 4. The energies of the three bandgaps associated with valence bands A, B and C are 3.445, 3.448 and 3.487 eV, respectively, at 4.2 K; see Rössler (1999). The ordering of the valence bands remains an issue of some controversy to this day, which is surprising given the rather basic nature of the question and the volume of published literature on the electronic and photonic properties of ZnO since the 1960's. To summarise this debate briefly, initial studies in 1960 of the excitonic reflectance

spectra of ZnO by D.G. Thomas (1960), combined with an accompanying theoretical analysis by J.J. Hopfield (1960) based on the "quasi-cubic" model of the O^{2-} 2p states yielded a satisfactory agreement between experiment and theory assuming a so-called inverted ordering of the top two valence bands compared to most other wurtzite semiconductors, i.e. the band ordering was found to be A - Γ_7, B - Γ_9, C - Γ_7. This inverted ordering is due, within the quasi-cubic model, to a negative spin-orbit coupling parameter compared to the free ion value; see Hopfield (1960). This apparent negative spin-orbit coupling parameter was subsequently explained as due to a small admixture of Zn d orbital character into the valence band wavefunctions, as described by Rowe et al. (1968) and Shindo et al. (1965). This is similar to the case of CuCl, which can alter the ordering of the top 2 levels due to the rather small value of the actual spin orbit coupling parameter in ZnO. However, subsequent measurements and analysis by Park et al. (1966) assigned the ordering as A - Γ_9, B - Γ_7, C - Γ_7, but this report erroneously identified the intrinsic A exciton reflectance and PL features with an extrinsic ionized donor bound exciton feature. These sets of measurements effectively began the valence band ordering debate. In the intervening years a number of theoretical and experimental contributions have appeared, with the majority supporting the initial conclusions of Hopfield and Thomas, including compelling evidence from Rowe et al. (1968) based on uniaxial stress studies of the bandedge reflectance spectra, though a number of papers have appeared relatively recently, both experimental and theoretical such as those by Gil (2001) and Reynolds et al. (1999), which continue to argue for the conventional ordering (Γ_9, Γ_7, Γ_7). However, the A - Γ_7, B - Γ_9, C - Γ_7 ordering is generally accepted in the community. A brief but thorough overview of this topic is given by Klingshirn (2007) in appendix A of his recent review. More detailed studies of the bandstructure have elucidated subtleties of the bandedge behaviour, including small k-linear contributions to Γ_7 symmetry valence bands along certain directions in the Brillouin zone (the effect is not seen for the conduction band); see e.g. Klingshirn (2007) and references therein. The effective masses of the carriers (including polaronic contributions) in ZnO are summarized in Rössler (1999), and in all cases (except the C valence band) these masses are close to isotropic ($m_{e,\perp,//} = 0.28\ m_0$, $m_{h,\perp,//,A,B} = 0.59\ m_0$, $m_{h,//,C} = 0.31 m_0$ and $m_{h,\perp,C} = 0.55 m_0$, with m_0 the free electron mass).

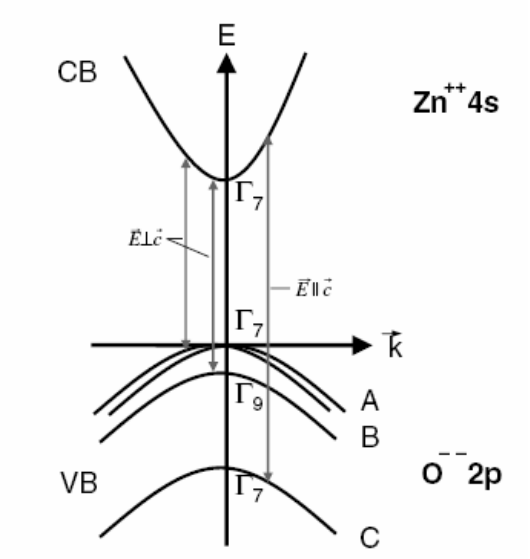

Fig. 4: Schematic diagram of ZnO band structure at zone centre. Image reproduced with permission from C. Klingshirn, "ZnO: From basics towards applications", Phys. Stat. Sol. (b), 244, 3027 (2007). Copyright 2007, Wiley-VCH Verlag GmbH & Co.

2.3 ZnO electrical properties

The study of the electrical properties of ZnO has been dominated to a large degree by the well-known and stubbornly persistent difficulty in doping the material p-type. Unipolarity is a common problem in many wide bandgap materials such as ZnO, GaN, CuCl, ZnSe, CdS and others. ZnO, grown in a nominally undoped state, generally displays significant n-type carrier concentrations (of the order of 10^{14} – 10^{17} cm^{-3} typically; see e.g. Look et al. (1998), Klingshirn (2007) and Ozgur et al. (2005) and the references therein). Related to this background n-type conductivity is the difficulty of type conversion of ZnO to p-type material by doping. This topic is probably the most extensively studied problem in ZnO research, and has played a major role in the evolution of the subject as commented upon in section 1 above. The decline in interest in ZnO as a photonic material in the late 1960's was undoubtedly due (at least in part) to the difficulties in p-type doping which led researchers to seek more fruitful materials as routes towards photonic devices. The doping studies on ZnO have concentrated mainly on thin films and although a number of interesting papers have looked to doping of ZnO nanostructures (attempting to exploit their high crystalline quality which is expected to lead to a reduced n-type background), the main interest in p-type doping remains in thin films. For these reasons only a very brief summary of the matter will be attempted. One consequence of the continued difficulties in doping ZnO p-type is that data for holes relevant to the electronic band structure such as masses and other electrical data such as hole mobilities are not known with nearly the same accuracy as the data for electrons and conduction band masses.

N-type doping of ZnO is rather easy by comparison with p-type. It is found that a range of group III elements, including Ga, Al and In, substitute for the Zn atom in the ZnO lattice and can lead to large, controllable, electron densities as discussed by Ozgur et al. (2005). N-type doping can be controlled to a sufficiently high degree that ZnO heavily doped e.g. with Al, is an attractive prospect for transparent conducting oxide (TCO) applications, which has been reviewed by Minami (2005). A summary of some of the electrical properties of electrons in ZnO may be found in the review by Ozgur et al. (2005).

To a large extent the difficulties with p-type doping of ZnO remain unfortunately as big as ever. These problems centre around (a) control and reduction of residual n-type background concentration; (b) identification of suitable shallow acceptors, whose solubility in ZnO and activation energies are appropriate for devices, where high doping levels (~ 10^{17} - 10^{18} cm^{-3}) are required in conjunction with reasonable carrier mobilities and (c) suitable introduction of these acceptors during (or post) growth. The control and reduction of residual n-type background concentration has proved challenging as it appears that the commonly observed native defects (such as oxygen vacancies, V_O, and zinc interstitials, Zn_i,) may contribute to this n-type behaviour. Like many other III-V and II-VI semiconductors, ZnO naturally tends towards a deficiency of the high column element, i.e. oxygen deficiency. The material can be significantly non-stoichoimetric due to growth or processing in a reducing (or just non oxygen-rich) environment. This oxygen deficiency leads to the formation of the associated V_O and Zn_i defects (though there have been significant divergences of opinion concerning which of these may be the dominant native defect). To add to the complexity of the situation, various

reports indicate that none of the native defects will occur in sufficiently high concentrations and/or with sufficiently low activation energies to account for many of the reported residual n-type carrier densities. A major step forward was made when it was suggested by van de Walle and other workers that H may be incorporated in ZnO (which can occur rather easily by diffusion during growth or processing, similarly to GaN) leading to large concentrations which can behave as shallow donors; see Van de Walle (2001) and Van de Walle (2000). It appears that this suggestion must play a sizeable role in explaining the residual n-type carrier densities seen. More recent work has also concentrated on various possibilities for H complexing with native defects and other impurities and the effects of this on doping as reported by Limpijumnong et al. (2004) and Börrnert et al. (2007).

Original research into identifying suitable shallow acceptors concentrated on following a parallel route to the n-type doping strategies, i.e. using group I elements substituting on the Zn lattice site. Elements such as Li and others do act as acceptors when substituting for Zn, but it is found that these impurities form rather deep acceptors with binding energies of hundreds of meV or even eV, which means that the fraction ionized at room temperature to create holes in the valence band is too small to enable device operation. However, doping by the use of group I elements has been used for many years to compensate residual donors to generate semi-insulating ZnO; see e.g. Hutson (1960). An additional problem with some of the group I impurities including Li and Ag, is that when doped in high concentration, they may behave as amphoteric defects, self-compensating the material; see. e.g. Lander (1960). More recent research work has concentrated on the use of group V elements substituting on the O lattice site as potential acceptors and elements such as N, P, As and Sb have been used. It appears that at least some of these elements have sufficiently low activation energies (N is reported to be ~ 100 meV) to make them suitable for device applications, as discussed by Look (2005). Other lines of research on this topic have looked at defect complexes as possible shallow acceptors; see e.g. Limpijumnong et al. (2004).

Finally the issue of suitable (i.e. reproducible and stable) introduction processes for these acceptors into the crystal structure has proven difficult also. A number of reports have appeared which seem to be once-off measurements often quoting exceptionally high p-type carrier concentrations, and the community has found these data hard to reproduce. There appear to be significant issues concerned with the medium and long term (days to months) stability of doped material. These include uncontrolled doping level changes and type conversion over such periods discussed by Lu et al. (2006) and issues relating to methodologies for reliable Hall measurements (whereby results appear to be affected by measurement environment including gas atmosphere and illumination conditions discussed by Schmidt et al. (2006)). Surface conduction effects and persistent photoconductivity appear to have important roles to play in a coherent interpretation of Hall data. These matters are topics of ongoing work and an overview of some of the problems is given by D.C. Look and co-workers in e.g. Look et al. (2005) and Claflin et al. (2007). However, a number of promising approaches to the problem of suitable incorporation of p-type dopants have also appeared. These include the idea of co-doping (see e.g. Zhang et al. (2001)) where n- and p-type dopants are introduced simultaneously into the crystal to yield defect complexes with high solubility and shallow acceptor behaviour, the repeated temperature modulation technique in

combination with laser molecular beam epitaxy (LMBE) where the substrate temperature is ramped between low temperatures (for N deposition to improve sticking coefficient) and higher temperatures (to enable high quality ZnO layer growth) reported by Tsukazaki et al. (2005) and most recently the suggestion of band engineering via the introduction of isovalent impurity complexes which alter the material bands and can enable shallow doping to such altered bands from existing acceptor levels as recently reported by Yan et al. (2007). The p-type data of Tsukazaki et al. (2005) are among the most promising published to date, but the excellent thin film material quality which appears to be at least partly responsible for these promising data is due in large part to the substrate used for thin film growth. The substrate in question, SCAM ($ScAlMgO_4$), is a rather rare material and the prospects for large area and large scale growth on this substrate are questionable. The topic of p-type doping as a whole has been characterized by a strong interplay between experimental work and theoretical modeling of defect complexes and predictions of likely p-type doping solutions. This interplay has been very fruitful by and large and the concepts of co-doping and isovalent impurity band doping represent good examples of where theory has usefully informed experiment and vice-versa.

The interplay and relative importance of the three aspects (n-type background concentration; identification of shallow acceptors and suitable introduction of acceptors) identified above as central to the p-type doping issue remains an open issue and whether universal solutions to this problem will be possible is as yet unclear. A number of authors have recently discussed aspects of the unipolarity problem in a more general way for a range of materials and the various contributions to the effect in different materials, though as yet generic experimental solutions remain a rather distant hope; see e.g. Lany et al. (2007) and Van de Walle (2006).

2.4 ZnO optical properties

ZnO shows pronounced optical absorption and emission in the near UV and blue regions of the spectrum, due to excitonic processes (both free and bound) and also shows defect-related visible and near IR emission at longer wavelengths. These characteristics have led to interest in the use of ZnO for optoelectronic devices such as LEDs and LDs, in addition to uses as a UV absorber for cosmetic and other uses. There is a long history of optical studies (both absorption and emission) on ZnO; see e.g. Heiland et al. (1959), Thomas (1960) and the review by Klingshirn et al. (2005). Thus the optical properties of the material are quite well established. Ellipsometry measurements have determined the values of the refractive index and the extinction coefficient over a rather wide spectral region for ZnO; see e.g. Schmidt et al. (2003) and references therein.

Given that the dominant interest in the optical properties of ZnO is based on absorption and emission in the blue / UV region associated with excitonic processes, we will concentrate on providing a brief overview of such processes. The direct bandgap of ZnO, and the fact that zone centre transitions between the conduction band and all the valence bands are dipole allowed means that this material is likely to show a strong interaction with optical photons. This is indeed the case. It is found that the binding energies of the free excitons associated

with electrons and holes from the A, B and C valences bands are very similar and equal to ~ 60 meV, with transition energies of ~ 3.376 eV, 3.382 eV and 3.421 eV, respectively as listed in Rössler (1999). The exciton Bohr radius is ~ 2 nm, as mentioned by Klingshirn (2007). The large exciton binding energy means that the free exciton state survives to temperatures above room temperature, and also survives in crystals and thin films of sub-optimal perfection implying that efficient excitonic emission processes may be expected in various optoelectronic emitters based on ZnO thin films and crystals.

The strength of the free exciton binding and the exciton-photon interaction means that the most useful starting point for a summary of the optical properties of ZnO is the mixed mode exciton-polariton. The energy and crystal momentum-conserving interaction between excitons and photons was first discussed independently and almost simultaneously by J.J. Hopfield in the USA and S.I. Pekar in the USSR; see Hopfield (1958) and Pekar (1958). Among the first material systems to which this new paradigm was applied were II-VI semiconductors such as ZnO, CdS and ZnTe, reported by Hopfield et al. (1960) and (1963). The relevant parameters characterizing the exciton-polariton in ZnO were determined based on experimental measurements of transmission, reflectance, photoluminescence, Raman scattering, multi-photon spectroscopies and other techniques; see Hopfield et al. (1965), Lagois (1977), Blattner et al. (1982) and Fiebig et al. (1993). These studies included the effects of spatial dispersion, and, in the case of reflectance measurements, the exciton dead-layer and additional boundary conditions (ABCs). The parameters are summarized in a number of publications for both ZnO single crystals and nanostructured thin films see e.g. Lagois (1977) and McGlynn et al. (2003). The exciton-polariton model has proven extremely useful in understanding almost all the optical properties of ZnO material under low levels of excitation, including CW and time-dependent PL; see e.g. Hauschild et al. (2006a) and (2006b).

At low light intensity levels single electron hole pairs, either in the exciton state or in the continuum, determine the optical properties as indicated above. However, as the pump intensity increases into an intermediate regime, the exciton density becomes sufficiently high to cause exciton interactions with other particles/excitations. Transitions involving exciton-exciton (ex-ex) emission may be observed which give rise to a large variety of optical nonlinearities as such processes will generally scale according to the exciton density squared (or higher powers). In bulk, single crystal ZnO at low temperatures (< 200K) under intermediate level excitations, a number of new optical emission bands appear, including the M-band, as discussed by Klingshirn (1975) and the inelastic scattering between an exciton and a free carrier, usually an electron in which the exciton recombines radiatively while the carrier is scattered to a higher state in its band; see Klingshirn (1975). In the intermediate excitation region at room temperature processes such as exciton-exciton (ex-ex) collisions become prominent due to the higher exciton density. This exciton-exciton collision process results in the recombination of one exciton and the emission of a photon with the remaining exciton promoted to an excited state, in a process analogous to Auger emission described by Klingshirn (1975). The exciton-exciton collision process will scale in proportion to the exciton density squared. The emitted exciton may be promoted into one of a manifold of excited states and the emitted photon will have a range of energies given by a simple hydrogenic model of the free exciton; see Klingshirn (1975) and Elliot (1957). This band is

known as the P-band, and the emission associated with such exciton-exciton collisions will generally be observed as a broad band centred ~90 meV below the free exciton emission.

When the pump intensity is increased further, exciton densities reach such levels that the excitons overlap and the exciton binding energy tends to zero, i.e. the exciton state becomes unstable. This high density regime is referred to as the Mott density, described by Klingshirn (1997). This is the result of a combination of physical processes, including the decrease of the band gap energy as a function of increasing carrier density (band gap renormalization), which can destabilise the exciton state compared to the free carrier state. Other important factors, at and beyond this Mott density, include phase space filling whereby occupation of the states near the band extrema, which are necessary to build up the exciton wavefunction, tend to saturate the exciton population. In addition, Coulomb interactions (due to screening of the Coulomb attraction between electrons and holes) will tend to saturate and quench the exciton optical signatures. The combined effects of such processes will destabilise the exciton state in favour of the free carrier state until eventually a new collective phase known as the "electron hole plasma" (EHP) results where an electron is no longer bound to a single hole to form an identifiable quasi-particle. These types of plasma phenomena are most easily observed in materials with large Bohr radii as described by Klingshirn (1997), but may also be seen in materials with a large exciton binding energy under more extreme conditions. Observations of the various nonlinear processes can be very different for different materials. For instance, in Ge the EHP can be seen under the illumination of an incandescent lamp due to the long life times of the carriers while the opposite is true for CuCl where an EHP is produced in the range ~ GW/cm^2 of pump intensity. II-VI semiconductors behave in an intermediate fashion, which allows observation of all the non-linear bands roughly simultaneously; see Klingshirn (1997).

In a material under sufficiently high levels of optical pumping, creation of population inversion, and thus both stimulated and spontaneous emission, can occur. As the system is pumped to higher and higher intensities, stimulated emission effects begin to dominate over spontaneous emission. In order for the material to lase an efficient feedback mechanism must be in place. In earlier studies of lasing in ZnO cavities were defined by e.g. stripe excitation geometries, while in more recent studies lasing has often been observed via the random lasing mechanism whereby the lasing cavities are "self formed" due to strong optical scattering and reflection at grain boundaries particularly in nanocrystalline thin films, but also in arrays of ZnO nanowires and other nanostructures and a recent review has been published by Djurisic et al. (2006) and the references therein. It appears based on the body of literature available that optically pumped ZnO, either in single crystal, thin film or nanostructured form, can be made to lase under both optical and electron beam excitation, using both conventional and random cavity formation.

At relatively low temperatures (compared to the lowest activation energy in the system being studied) under excitation the free carriers or free exciton-polaritons can be trapped at defects in the crystal and remain in such metastable defect states before photon emission, with a photon energy characteristic of the defect in question. This defect-related emission is a very powerful tool for characterization of material properties, purity, defect species. This has led to

many optical studies of point and other defects in these materials for the purpose of understanding the nature of these defects and, particularly, their effects on doping; see e.g. the review by Meyer et al. (2004). Comparisons of experimental results with theoretical predictions of defect structures have been reported. In addition, important recent (and more established) results indicate that effective routes to p-type doping in ZnO may rely primarily on defect complexes rather than isolated substutional defects, see e.g. Limpijumnong et al. (2004), and this may explain the rather checkered history of success of p-type doping methods in ZnO. The defect-related emission from ZnO can be conveniently (if rather arbitrarily) divided into shallow (i.e. close to the bandedge energy) emission which is generally associated with emission from a range of defect-bound excitons, and defect complexes such as donor-acceptor pairs and deeper level emission from other defects and defect complexes. The shallow emission is generally sharp and its fine structure can often be understood on the basis of perturbed excitonic models using the effective mass approximation. Such emission can be studied at high resolution in great detail and used as a very sensitive probe of the material and its defect content and is sensitive to temperature, strain, electric and magnetic fields, isotopic mass and many other potential perturbing influences. By contrast the deep level emission is often quite broad and rather featureless and identification of the microscopic defect(s) responsible for such emission can be a frustrating and time-consuming task.

Among the earliest classifications of shallow near bandedge PL lines in ZnO was by Tomzig et al. (1976) whereby the band edge PL in bulk ZnO is divided into seven regions: (a) free exciton (3.3765eV < FE < 3.3925eV); (b) excitons bound to ionised donors (3.3646eV < D^+X < 3.3765eV); (c) excitons bound to neutral donors (3.3605eV < D^0X <3.3646eV); (d) excitons bound to neutral acceptors (3.3536eV < A^0 < 3.3605eV); (e) exciton bound to deeper centers (3.3329eV < E < 3.3536eV); (f) two-electron transitions (3.3151eV < E < 3.3329eV); (g) phonon replica region (E < 3.3151eV). The regions D^+X, D^0X and A^0 are known collectively as the Bound Exciton Complex (BEC) region. These regions taken from Tomzig et al. (1976) are not exact, with differences e.g. in the measurement temperature causing a degree of blurring of the boundaries. However they are used as a starting reference point in the assignment of the bands. The categorisation of regions by Tomzig et al. (1976) was based upon Haynes rule, which relates the binding energy of the exciton to the neutral complex to the binding of the additional carrier to the point defect using a value of Haynes' constant of 0.1 for both donors and acceptors based on theoretically predicted values for II-VI compounds reported by Halsted et al. (1965). Recent experimental studies however have found the Haynes' constant to be ~ 0.37 for both donors and acceptors; see Schildknecht et al. (2003). These data along with other considerations have led to a re-evaluation of the bound exciton assignments as discussed by e.g. Gutowski et al. (1997) and by Klingshirn (1997). More recent studies have utilised the so-called I-line classification scheme to categorise the near band edge bound exciton complexes, all of which are assigned to donors, and many of which have been definitively associated with particular defects and chemical elements. The details of bound exciton spectra and the I-line assignments are comprehensively covered in the review by Meyer et al. (2004).

The deeper level emission, as mentioned above, is generally broader and thus more difficult to conclusively assign to a specific microscopic defect (though not always,

particularly at low temperatures; see for example work on ZnO:Fe discussed by Heitz et al. (1992) and also the sharp zero phonon line emission from ZnO:Cu discussed by Dingle (1969)). Broad emission bands in the blue, green, orange and red spectral regions, in many cases occurring simultaneously, have been identified. These bands are often affected by Fabry-Perot fringes due to interference in thin film samples making their separate identification even more challenging. Of these, the so-called "green band" with a maximum emission at ~ 520 nm discussed by Vanheusden et al. (1996) is the most commonly seen deeper emission at room and low temperatures. This band has been assigned most consistently to an oxygen vacancy as reported by Vanheusden et al. (1996) and Leiter et al. (2003).

2.5 Further ZnO materials properties

ZnO displays a range of other interesting materials properties, including the potential for magnetic behaviour when doped with various impurities as discussed by Ozgur et al. (2005)), piezo-electric behaviour, discussed by Hutson (1960), Bateman (1962) and Crisler et al. (1968); (persistent) photoconductivity discussed by Hirschwald (1985) and Liu et al. (2004); surface conduction discussed by Schmidt et al. (2006), Look et al. (2005) and Claflin et al. (2007); catalytic and photocatalytic activity discussed by e.g. Woll (2007) and Ameta et al. (2003) and field emission discussed by Fang et al. (2008)). Section 5 will outline some applications of ZnO nanostructures where the ZnO morphology in conjunction with some of the properties listed above provide interesting possible application areas for such structures. The applications which will be discussed are (a) electrical, optical/photonic applications relying on the properties discussed in sections 2.1 – 2.4 above; (b) field emission applications and (c) applications in sensing, energy production, photochemistry, biology and engineering.

3. GROWTH OF ZNO NANOSTRUCTURES

3.1 General comments

The growth of ZnO nanostructures may be undertaken by a variety of methods, including nearly all the common growth techniques such as vapour phase transport (VPT), chemical vapour deposition (CVD), molecular beam epitaxy (MBE), pulsed laser deposition (PLD), sputtering and chemical solution (CS) methods. A large number of reports on ZnO nanostructure growth have been published for each of these methods and a large diversity of nanostructure morphology has been reported, both within any specific growth method and from method to method. In addition, there is a wide variation in these reports of growth parameters used such as temperature, gas pressures and composition, flow rates etc. These will all tend to affect key growth parameters such as substrate and vapour temperatures, vapour supersaturation, ad-atom and vapour phase diffusion and kinetics of film formation via e.g. Zn oxidation reactions. The exact growth conditions then affect the sizes (diameter, lengths) and growth modes (nanorods, nanowires etc.) of the deposited material. Because of the quantity and diversity of such reports and the difficulty (or even impossibility) of inter-comparison it seems in order to make some preliminary comments concerning general aspects of the process.

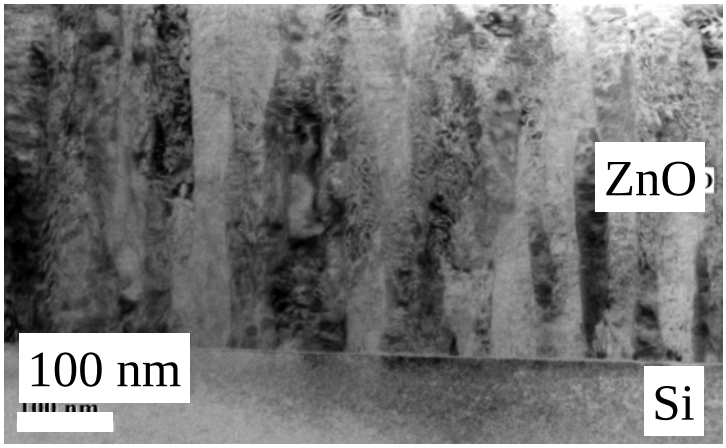

Fig. 5: Cross-sectional TEM data of PLD-grown ZnO thin film on Si substrate, showing columnar nature of film (TEM data courtesy of Dr. Simon Newcomb, Glebe Laboratories, Tipperary, Ireland).

The first point worth noting is that ZnO tends naturally to grow in a nanostructured form under many conditions as mentioned in section 1. High aspect ratio ZnO needles (with hexagonal cross-section) seem to be a common morphology for ZnO crystals with a range of diameters from the macroscopic to the nano-scale; see e.g. Wang (2004). This type of structure is consistent with the symmetry of the ZnO lattice and in some cases (particularly for slow growths and large crystals) the crystal obtained may be indicative of the equilibrium crystal habit of the material in the particular circumstances with substantially different growth rates along the polar, prismatic and pyramidal faces as discussed by Laudise et al. (1960). However, in many cases of nanostructure growth the crystallite shape is not indicative of the equilibrium crystal habit and the growth process is clearly affected both by the thermodynamic/energetic aspects of the process and the kinetic aspects, and both these aspects can be strongly affected by the nature of the substrate upon which growth is performed. Even in the case of ZnO thin films the tendency to grow in nanostructured form is often evident, with transmission electron microscope (TEM) data and other techniques showing that in many cases such films are formed of many crystallites elongated along the c-axis and stacked with their c-axis normal to the substrate, in effect a very dense field of nanorods. An example of this behaviour is shown in figure 5 for ZnO thin films on Si. The complex interplay between these two aspects must, in the present authors' opinion contribute to the diversity of nanostructure morphology observed in practice. This hypothesis is strengthened when one considers the growth of structures such as ZnO nanotetrapods and nanoflowers, where the morphology is clearly not consistent with the ZnO crystal habit and must be due at least in part to kinetic aspects of growth. The majority of papers dealing with ZnO growth are experimental in nature, and the amount of theoretical work is rather limited. Among the main recent contributions to the theoretical effects have been the work of A.S. Barnard and colleagues, who have considered the formation of ZnO nanostructures theoretically based on thermodynamic issues, and including the effects of surface energies, in addition to the effects of impurity incorporation; see e.g. Barnard et al. (2006) and Fan et al. (2007). These works have opened a new avenue in ZnO nanostructure research and have helped shed light on interesting experimental results concerning the observed changes in nanostructure morphology due to In contamination as discussed by Fan et al. (2007). However, the absence to date of a comprehensive study of both the thermodynamic and

kinetic aspects of the growth process is a major gap in this field and one which will very significantly hinder fundamental scientific understanding of the process and thus ability to control and reproduce nanostructure growth (particularly on large area substrates). One is drawn to make some comparisons and analogies with the case of another hexagonal symmetry crystal which can form a wide range of structures due to relatively small variations in growth parameters, i.e. ice, in the form of snow-flakes, discussed in the review by Libbrecht (2005). In the case of snowflake formation, many similarities to ZnO nanostructures may be pointed out, including the hexagonal crystal symmetry, which is often (but not always) reflected in the snowflake symmetry and the extreme sensitivity to both temperature and water vapour supersaturation. Clearly there are differences also, notable amongst which is the fact that the H_2O molecule exists as the stable gaseous species whose condensation leads to crystal growth whereas in the case of ZnO most evidence would suggest that ZnO molecules exist at a very low concentration in the gas phase (in nearly all vapour or molecular beam growth methods) and that growth is dominated (though perhaps not nucleation) by Zn vapour attachment to the surface and subsequent reaction with oxygen. However, the point being made is that, just as in the case of snowflakes, any attempts to understand the morphologies observed must be guided by both thermodynamic and kinetic aspects.

For the reasons mentioned above, the overwhelming majority of work on ZnO nanostructures is based on bottom-up, self-organisation of the various nanomorphologies which form and whose shape can be tailored and controlled by control of growth parameters. Work on top-down, lithographic definition of ZnO nanostructures is very much less explored, though hybrid approaches, where some pattern definition of e.g. substrates, is used to seed ZnO growth is sometimes found as reported by Fan et al. (2006). The clear advantage of the bottom-up approach is the element of self-organisation and the lack of expensive lithographic processing steps. The disadvantages include the high sensitivity of the nanostructure morphology to a number of growth parameters, meaning that nanostructure length, diameter, positioning and spacing are all quite variable (far more than would be tolerable in top-down processes) and this may lead to significant disparity in size and structure for rather similar growth conditions. However, for some applications, the dispersity in e.g. nanorod diameter is less important than the advantages the self-organisation offers. In the case of arrays of nanorods for photonic applications, the crystal and optical qualities associated with the nanorod morphology far outweigh any disadvantages in terms of variability of diameter when the average diameters are ~ 100 nm. Such variation does not lead to appreciable spectral broadening because quantum confinement effects are only seen for structure diameters close to the exciton radius of ~ 2 nm (as mentioned in section 4.2 below). Thus in many cases the self-organisation of nanostructures offers many materials advantages without the obvious disadvantages being especially deleterious.

Figure 6 below is a reasonably crude qualitative attempt to summarise the present authors' overview, listing the various aspects of the ZnO nanostructure growth process which must be of some importance. The discussion below will then attempt to comment on the degree to which the various aspects are known. It is thus an attempt to modularize the steps of the process which may make them amenable to future individual investigation or investigation in blocks. It should be emphasized that there is little or nothing of great novelty in the figure or

the overview, in the sense that similar overviews for growth of III-V films by MOCVD exist and many other examples of materials growth in different systems have been described by similar diagrams to be found in e.g. the textbook by Smith (1995).

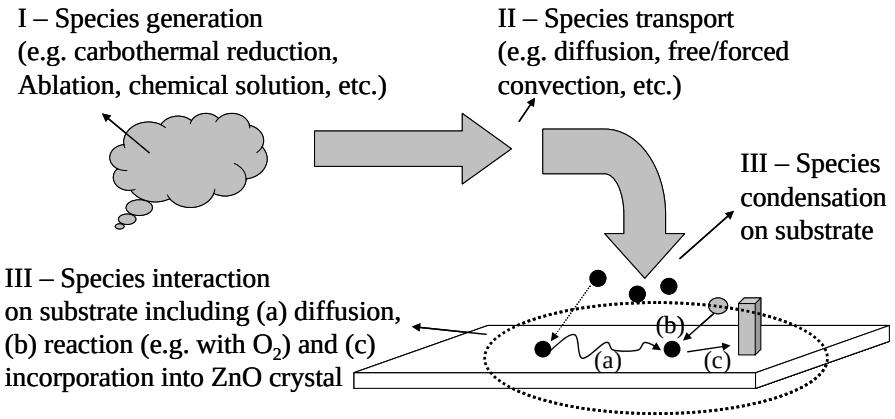

Fig. 6: Schematic diagram summarizing the stages of ZnO nanostructure growth.

The first stage of the process is the generation of the constituent materials, which in the case of ZnO growth seems to be a mixture of Zn-containing species and oxygen-containing species in all cases. The generation of these species is performed differently in different techniques and these will be discussed in some more detail in sections 3.2 – 3.5 below. The temperatures and partial pressures/concentrations at which these species are generated are the first two adjustable parameters for ZnO growth. There do not seem to be many recorded cases where the main growth mode of ZnO involves the condensation of a ZnO-containing species from the source (with the exception of CS methods and the possible exception of PLD, see section 3.3 below). This is very understandable for vapour and molecular beam methods. The ZnO molecule is unstable in the vapour phase relative to the Zn and O_2 species, and is characterized by a positive Gibbs free energy of reaction of at least 30 kJ/mol at 1000^0C (given in the tables of thermochemical data by Pedley et al. (1983)), though in many cases this is inferred from lower detection limits (which give a dissociation energy of ~ 2.77 eV for the gaseous ZnO molecule) indicating the actual value of the dissociation energy may be much lower and thus the Gibb's free energy of reaction may be much higher. This is supported by first principles calculations such as the work by Gusarov et al. (2006) which predicts a dissociation energy for the ZnO molecule of ~ 1.7 eV. This leads to a positive Gibbs free energy of reaction of ~ 270 kJ/mol at 1000^0C, according to calculations performed by Saunders (2008). These considerations mean that the concentration of the ZnO molecule in the vapour phase will be at most ~ 5% that of the Zn and O_2 species (assuming a Gibb's free energy of reaction of 30 kJ/mol) and possibly as low as one billionth the concentration of the Zn and O_2 species (with a Gibb's free energy of reaction of 270 kJ/mol). Hence the growth rates due to direct ZnO vapour condensation one would expect on the basis of such concentrations are likely to be very small and in all likelihood negligible. However, it must also be noted that the ZnO molecular vapour, even though at very low concentration relative to Zn and O_2 may in fact be supersaturated relative to the substrate downstream, even if the

Zn vapour is not. Hence on certain substrates, the ZnO vapour may play a role in initial nucleation steps to create a small number of ZnO nuclei on which Zn vapour may subsequently condense to form larger ZnO structures. This may be especially important on substrates which do not offer energetically favourable sites for Zn condensation and when Zn vapour supersaturation is low (e.g. uncatalysed SiO_2 at relatively high temperatures) and evidence in support of this suggestion has been reported many years ago during studies of the growth of Zn thin films on quartz by Forty (1952). It is likely that this stage of the process may be described by thermodynamic principles with a reasonable degree of accuracy for most growth methods.

The second stage of the process is that of species transport from the source region to the substrate. Again there are significant differences between the various growth methods with regard to this stage. In a technique such as MBE this stage is likely to be rather uncomplicated, whereas the processes of diffusion and free and forced convection which operate in techniques such as CVD, VPT and CS will have a strong influence on the material transport kinetics from source to substrate. Issues such as carrier gas presence, pressure, flow rate and possible reactivity will all play a role (though for the most part inert gases are used as carriers) in determining the material flux to the substrate as will diffusion and boundary layer effects at the substrate surface. At present it is also an important open question as to what extent the morphology of the ZnO nanorods grown by vapour phase techniques at pressures close to atmospheric are affected by the Berg (1938) effect which is known to operate in systems where dendritic and other complex growth morphologies are determined by diffusion limited growth effects, known to be important for growth of snowflakes, discussed by Libbrecht (2005) and (2008)). The smaller dimensions of the ZnO nanostructures and the fact that they often grow rather tightly packed on planar substrates means that it will not be possible to treat individual nanostructure growth and its interaction with the source vapour in

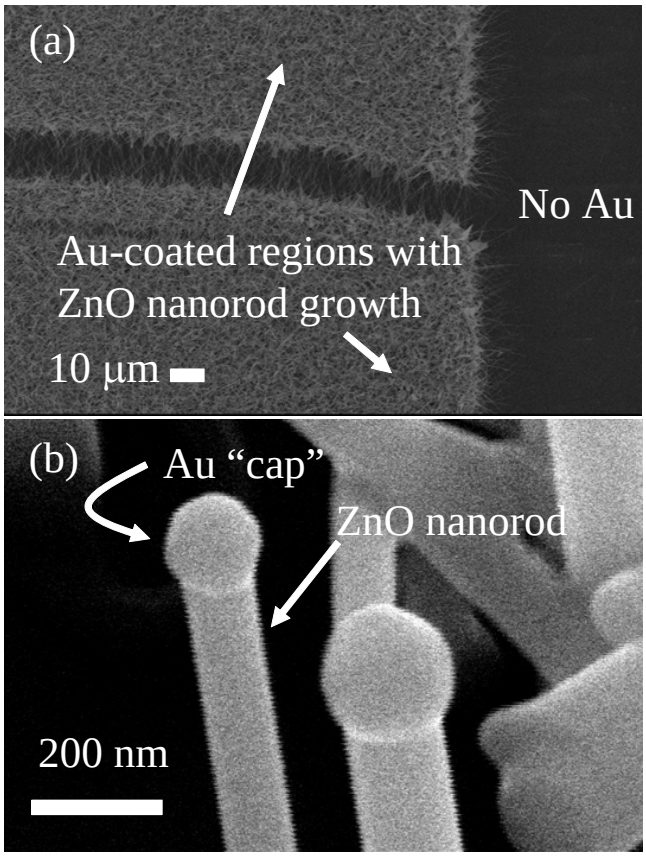

Fig. 7: SEM images of ZnO nanorods grown by VLS method on a Au-coated Si substrate at various magnifications. Selective growth on Au-coated regions is seen in (a), while the Au "caps" on the nanorod ZnO tips are shown in (b). Data courtesy of Drs. K.K. Nanda and J. Grabowska.

isolation from the effects of close neighbours; see Libbrecht (2005). This stage of the process will be largely determined by growth kinetics, operating over a range of length scales. Furthermore, the overall chamber pressure may have a significant effect on the nanostructure morphology, and this has been observed by a number of authors for pressure changes in the range 1 – 1000 mbar; see e.g. Park et al. (2005) and Song et al. (2005). It is important to note that the molecular mean free paths change from ~ 50 nm at 1000 mbar to ~ 50 μm at 1 mbar as described in Chambers et al. (1998). The alteration of the mean free path will naturally affect the important growth parameters such as gas diffusion and boundary layers and it is important that the range of pressure over which substantial morphological changes are observed correspond to changes in molecular mean free path from substantially smaller than typical ZnO nanostructure long axes (the typical nanorod/nanwire lengths are ~ 5 – 10 μm) to greater than those typical dimensions. This is quite different to the situation existing for the growth of snow crystals at atmospheric pressure.

The third stage of the growth process is the impingement of source species on the substrate, effectively the condensation of the source species. This stage of the process is significantly affected by the nature (chemical and structural termination) of the substrate and its temperature. The substrate temperature in combination with the source concentration effectively determines the supersaturation, i.e. the driving force for nucleation of source material on the substrate from the surroundings (for vapour phase and molecular beams this is most probably Zn-containing species based on the discussion above). For growth from the vapour phase at relatively high substrate temperatures (800^0C – 900^0C) which implies a low Zn vapour supersaturation) on bare and relatively unreactive substrates such as SiO_2 and Al_2O_3 only very low growth rates are observed if growth is seen at all; see e.g. Kim et al. (2003b) and Zhao et al. (2004). Furthermore, the growth, when observed, in such conditions is often rather random, with no well-defined texture. By contrast, growths on Si substrates using MOCVD at lower substrate temperatures (~450^0C – 600^0C, which implies a higher supersaturation) can proceed, as discussed by Park et al. (2002a) and (2002b)). These observations incline one to the view that different mechanisms control the growth, perhaps with Zn-species vapour condensation and subsequent oxidation dominating at low growth temperatures. Slower deposition of ZnO nuclei followed by subsequent growth around such sparse nuclei may be the mechanism by which the higher temperature growth proceeds. At low supersaturation the condensation coefficient for Zn vapour on such substrates is rather low. Both these mechanism correspond to vapour-solid (VS) growth.

In order to enable effective growth of ZnO nanostructures on such nanoreactive substrates at high temperatures it is necessary to increase the condensation coefficient for Zn vapour and this is generally accomplished by the use of metal catalysts (such as Au nanodots, see e.g. Yang et al. (2002)) to provide preferential accommodation sites for Zn vapour nucleation even at low supersaturation.

Significant growth rates are seen on such substrates only on regions with Au layers deposited, as shown in figure 7. In the case of Au-catalysed substrates two growth mechanisms may proceed after Zn vapour condensation, firstly the so-called vapour-liquid-solid (VLS) growth whereby the adsorbed Zn can form a eutectic molten solution with Au

nanodrops on the surface, with subsequent supersaturation, precipitation and oxidation to form ZnO nanorods with characteristic Au “caps” at their tips (shown in figure 7 and described by Yang et al. (2002)). A VS mechanism may also operate whereby Zn vapour condenses at locations coated in Au (although the VLS mechanism does not operate) and oxidizes to form ZnO nanostructures; see Li et al. (2006). The VLS process can operate in parallel with the VS mechanism over a finite temperature interval according to recent data from our group (Rajendra Kumar et al. (2007a)), thus allowing us to definitively distinguish the processes of nucleation at Au nanodots and subsequent participation in either the VLS or VS mechanisms. A number of authors also discuss a so-called self-catalysed VLS mechanism with Zn droplets at the ZnO nanorod tips but the ZnO certainly does not play the same role as Au does (or other metals) in traditional VLS and it does not appear to the present authors that a clear distinction can be made between this growth mechanism and traditional VS; see e.g. Wang et al. (2003) and Wei et al. (2005).

By contrast, no Au droplets are needed for vapour phase growth on ZnO buffer layers, even at high substrate temperatures, implying that the ZnO surface can provide energetically suitable sites for Zn nucleation, thus increasing the condensation coefficient for Zn vapor (at least for certain ZnO facets, see Rajendra Kumar et al. (2007b)). The relative condensation coefficients for Zn on the various basal, prismatic and pyramidal facets of ZnO are not very well known, at least in the non-UHV environments in which nanostructure growth normally occurs. However, it seems clear that there are significant variations both with facet and temperature, which lead to the highly anisotropic growth morphologies seen in experiments, and it appears that in many (though not all) cases the growth along the *c*-axis direction is fastest; see Wang (2004). This stage of the process will be controlled predominantly by thermodynamic factors (with respect to issues such as supersaturation and eutectic melt formation in VLS).

The final stage of the process involves other interactions with the substrate including diffusion across the surface, re-evaporation and finally incorporation of species into the crystal. These stages of the process will be controlled by a delicate balance of thermodynamic (with respect to issues such as diffusion coefficients and barriers) and kinetic (such as reaction rate) factors. The effects of diffusion barriers such as Schwoebel barriers (described by Pimpinelli (1998)) on ad-atom motion and the consequences for the morphological evolution of ZnO nanostructures are little known in the typical growth environments used. In addition to factors such as diffusion across the surface (or through Au dots in the VLS mechanism) to appropriate locations to incorporate into the crystal, an important step in this final stage is the reaction of Zn-containing species with O-containing species to form ZnO. In the vapour phase this reaction is reported to have a reaction rate characterized by an activation energy of ~ 0.73 eV, reported by Kashireninov et al. (1982). An activation energy of similar order of magnitude (or less) is expected for Zn oxidation on a foreign substrate. Both these final factors will be determined by the substrate temperature and the effects of temperature on diffusion and re-evaporation will compete with temperature effects on the $Zn + O_2$ reaction rate. The combination of these effects ensures that the final stage of crystal growth is controlled by a balance of thermodynamic and kinetic factors.

The substrate structural and chemical termination effectively determines whether the nanorods grow in an epitaxial manner or in a disordered, polycrystalline manner. Growth on Si substrates is generally observed to show no in-plane order, which is consistent with the presence of an amorphous SiO_2 interface layer reported by Cheng et al. (2005). Growth on Si is also often observed to be untextured (e.g. nanorods not aligned preferentially normal to the substrate), although low temperature MOCVD growth has shown examples of textured nanorod arrays, which supports the earlier assertion that a different mechanism dominates in such circumstances; see Park et al. (2002b). Growth on sapphire, particularly *c*-plane and *a*-plane sapphire, where lattice-matching and domain matching conditions exist, is generally epitaxial and in many cases well-aligned arrays of nanorods are seen over areas of 10's of μm^2, as shown in figure 8 above; see also Grabowska et al. (2005). Growth on other substrates such as glass, quartz, alumina, plastic and metal often shows texture at very low growth temperatures (due to the high surface energy of the ZnO basal planes as reported by Greene et al. (2005)) and random growth at higher temperatures as reported by Huang et al. (2007).

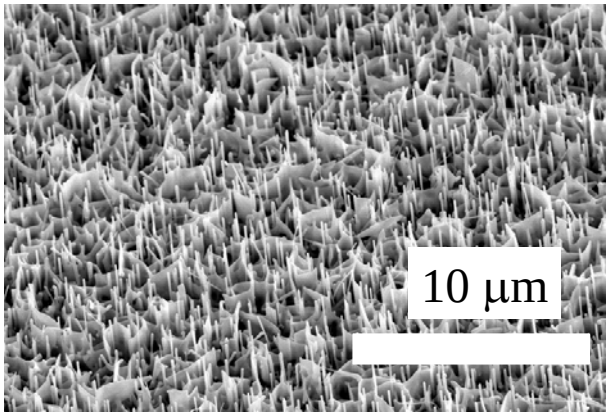

Fig. 8: SEM image of ZnO nanorods and nanowalls grown on *a*-plane sapphire. Data courtesy of Drs. K.K. Nanda and J. Grabowska.

The growth of ZnO nanostructures, when viewed across the literature as a whole and taking into account the summary overview above, is described by a great number of (not necessarily independent) parameters. While many aspects can be well described by classical growth theory of the type treated in the Burton, Cabrera and Frank (BCF) model (see e.g. Pimpinelli et al. (1998) and the references therein), there are also additional complexities associated with e.g. the nucleation. For example, for growth on almost all substrates, even at conditions indicative of low supersaturation, there is no evidence that all or even most nanowires contain dislocations, as discussed in section 4.1 below, or in general that they initially nucleated at dislocation or other regenerative defect sites on the substrate. The presence of Au nanodots (probably in liquid form or surface-melted) or appropriate sites on planar ZnO surfaces (e.g. O-terminated planes) appear to provide suitable nucleation sites even in the absence of defects in the majority of cases.

The following sections will attempt to briefly summarise a selection of the main techniques used for growth of ZnO nanostructures.

3.2 VPT and CVD methods

VPT methods are among the most popular growth techniques for growth of ZnO

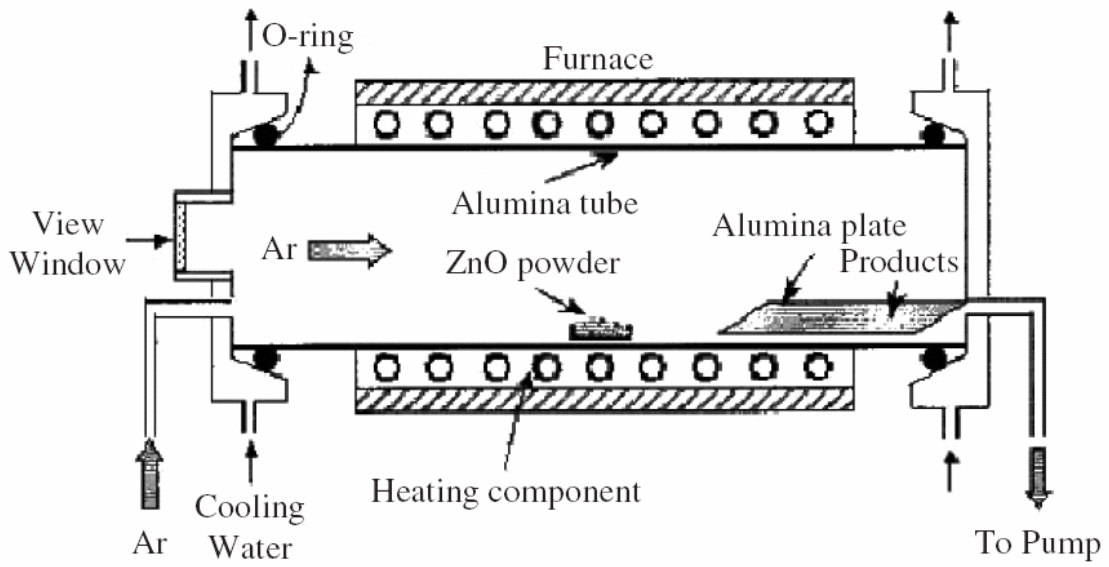

Fig. 9: Schematic diagram of VPT apparatus used for ZnO nanostructure growth using ZnO powder as source. Image reused with permission from Z.L. Wang, J. Phys.: Condensed Matter, 16, R829 (2004). Copyright 2004, Institute of Physics Publishing.

nanostructures and VLS growth using VPT was one of the first methods used to grow ZnO nanorods during the "modern" era; see Yang et al. (2002). In VPT, the source vapour may be generated either by (a) direct evaporation of Zn metal as reported by Park et al. (2006), (b) carbothermal reduction of ZnO powder using graphite or activated carbon powders as reported by Yang et al. (2002) or (c) direct congruent sublimation of ZnO powders as described by Wang (2004). Each of these methods is associated with a different temperature range, with Zn metal evaporation proceeding in the temperature range < 800^0C. Carbothermal reduction is determined by the Ellingham diagram and generally proceeds in the temperature range 850^0C – 1000^0C, while ZnO sublimation proceeds at higher temperatures (> 1200^0C). A schematic diagram of a VPT system is shown in figure 9. The source powder temperature controls the Zn source vapour pressure, while the sample temperature controls supersaturation. These can be controlled independently either by using a two (or more) zone furnance, or by varying the source-sample separation in a single zone furnace and using the temperature profile of the furnace. The vapour flow may be controlled by an adjustable argon gas flow. The oxygen source may be either the residual oxygen in the chamber or oxygen may be introduced separately; see e.g. Reiser et al. (2007). The Wang group in the Georgia Institute of Technology has used VPT growth at higher temperatures (1200^0C) via ZnO powder sublimation to generate a number of very interesting new "families" of ZnO nanostructures, including nanobelts, nanospirals and nanohelices, whose structure appears to be controlled by the effects of the surface charges of the polar ZnO basal faces, and comb-like ZnO nanostructures which show dendritic secondary growths on certain ZnO facets and not on others; see the reports by Wang (2004) and Wang et al. (2003). A small selection of these structures was shown in figure 2 earlier.

CVD methods, and in particular MOCVD has been used extensively to grow ZnO nanostructures, and in particular has been an effective tool for the growth of ordered arrays of ZnO nanorods on e.g. Si and sapphire substrates as reported by Park et al. (2002a) and (2002b). The most common metal organic source been used for MOCVD growth of ZnO nanostructures appears to be diethylzinc (DEZn) reacting with oxygen gas, reported by Park et al. (2002a), although Zn halide sources such as $ZnCl_2$ have also been used, reported by Xu et al. (2004) in addition to combustion of zinc nitrate with methane, reported by Liu et al. (2005). The ability to grow samples of nanorods with excellent uniformity and texture, in combination with the ability to alter the gas composition in MOCVD, has enabled the group of G.C. Yi in POSTTECH in Korea to engineer nano-heterostructures into nanorods to create quantum dot structures of high structural perfection, reported by Park et al. (2003), an example of which is shown in figure 10.

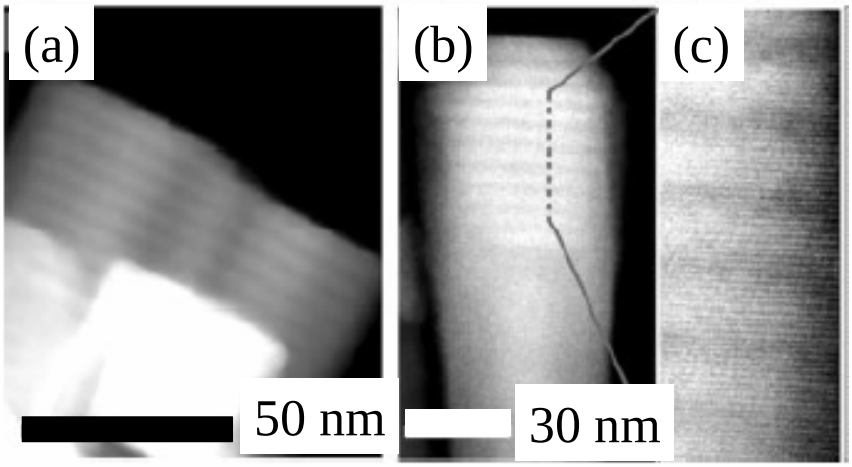

Fig. 10: TEM images of ZnO/ZnMgO nano-heterostructures grown by MOVPE. Images reproduced with permission from W.I. Park, "Quantum Confinement Observed in ZnO/ZnMgO Nanorod Heterostructures", Advanced Materials, 15, 526 (2003). Copyright 2003, Wiley-VCH Verlag GmbH & Co.

ZnO nanostructures grown by VPT and CVD show excellent optical and electrical properties for the most part, with narrow bound exciton emissions in low temperature PL data and TEM data showing single crystallinity in many such nanostructures.

3.3 MBE, PLD and sputtering methods

Physical vapour deposition methods including MBE, PLD and sputtering methods have also been used by a number of groups to grow various nanostructures; see e.g. Tien et al. (2007), Kumar et al. (2007), O'Haire et al. (2006) and Lorenz et al. (2005). Among these, PLD has been used to produce a rather large variety of nanomorpholigies by a number of groups including the Leipzig group and our own group, see O'Haire et al. (2006) and Lorenz et al. (2005), some examples of which are shown in figure 2. In PLD, either a ZnO pressed powder target or a Zn metal target may be used as a source. In most cases, even when using a ZnO target, excess oxygen is required to ensure stoichoimetry of the ZnO material grown and thus an oxygen ambient of some mbar pressure is used in all cases. The exact growth

mechanism of nanostructures during PLD remains unclear, however the transition from uniform thin films to nanostructures appears to correlate well in some cases with an increase in the chamber pressure as reported by O'Haire et al. (2006). In turn this may imply that ZnO nanoparticulate nucleation is beginning in the laser plasma plume in the growth regime leading to nanostructures, which is a very different growth mechanism to that which seems to operate in VPT and CVD, as discussed above. Once again, ZnO nanostructures grown by physical vapour deposition methods generally display excellent optical and electrical properties in PL and TEM experiments and the control available is sufficient to enable nano-heterostructures engineering into nanorods, as shown recently by Czekalla et al. (2008).

3.4 CS Methods

One of the characteristics of the growth methods discussed in sections 3.2 and 3.3 above is the fact that the substrate temperature in all cases is rather high (400^0C or even more in many cases). The many promising materials qualities of ZnO, such as potentially excellent optical efficiency, mean that many researchers are keen to combine these qualities with as diverse a range of substrates as possible, including flexible plastic substrates for integrated flexible optoelectronic and photonic applications. However, it is either difficult or impossible to use growth temperatures of 400^0C or higher in conjunction with flexible plastic substrates without destroying the substrates. Thus, in the last number of years, many workers have explored the possibility of using low temperature ($< 400^0$C and even $< 100^0$C) CS methods; see Greene et al. (2006). These methods include the use of chemical solutions such as the hydrolysis of zinc nitrate in water with the addition of hexamethylenetetramine or the decomposition of zinc acetate in trioctylamine; see e.g. Greene et al. (2005) and Greene et al. (2006). The ZnO nanostructures grown in this way may show a range of morphologies depending on the growth conditions as reported by Postels et al. (2007) and Bai et al. (2008) but in many cases arrays of well-aligned closely spaced nanorods of thicknesses ~ 200 – 300 nm are found, regardless of the substrates type as discussed by Greene et al. (2005), and these structures are useful for various devices such as LEDs and field emitters (see figure 11 and sections 5.1 and 5.2 below). The origin of this growth mode seems to be associated with two effects. Firstly the low growth temperature means that the energetics of the ZnO crystal and specifically the high surface energy of the ZnO basal planes may dominate and the ZnO (0001) plane will align parallel to the surface locally to reduce the free energy of the system. Secondly, the rather close packing and higher thicknesses of the nanorods (compared e.g. to

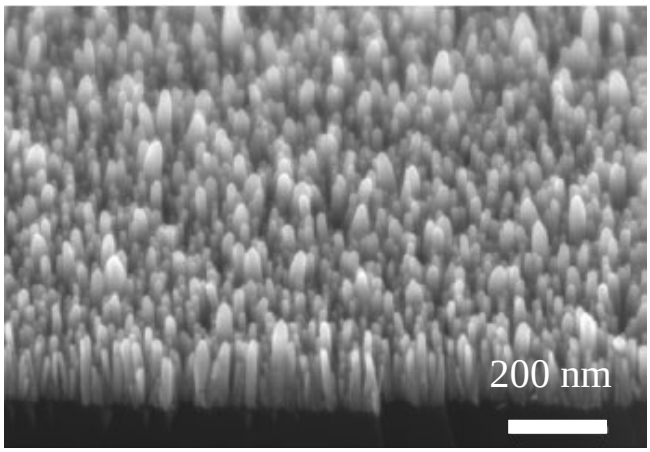

Fig. 11: SEM image of vertical nanowire arrays on silicon. Image reprinted with permission from L.E. Greene, Nano Letters, 5, 1231 (2005). Copyright 2005, American Chemical Society.

VPT) may lead to mechanical stresses during growth if nanorods grow into each other. These stresses will be eliminated by a growth mode with the nanorod *c*-axes normal to the substrate and thus as the nanorod grow longer this growth mode may be favoured and eventually dominate as reported by Postels et al. (2007).

In all cases the authors know of, the structural properties of CS-grown ZnO nanorods are good and single crystal nanostructures such as nanorods are seen, but the optical properties, specifically the PL properties, are significantly degraded with respect to e.g. VPT-grown nanostructures. This is seen in a number of aspects of the PL, including very strong defect band emission compared to the bandedge emission, but also (and more tellingly) large bound exciton linewidths in low temperature PL (~ 10 meV) which mean that individual members of the I-line series cannot be resolved; see e.g. Bekeny et al. (2006). The optical properties can be recovered to an extent by annealing treatments in oxygen-rich environments (to restore the bandedge emission intensity), but the linewidths do not recover to the sub-meV values associated with nanostructures grown by other methods such as e.g Grabowska et al. (2005). The origin of this deterioration of optical properties is probably inextricably linked to the key advantage of the CS method – i.e. low temperature growth and it is hard to see how this problem can be overcome, especially as annealing will tend to bring about the same problems as high temperature growth in terms of flexible substrate degradation.

4. ZNO NANOSTRUCTURE CHARACTERIZATION

4.1 Structural characterization (including SEM, XRD, TEM)

Structural characterization of ZnO nanorods has been undertaken using a variety of methods particularly SEM. This is the workhorse imaging tool for visualization of ZnO nanostructures and the typical dimensions of such structures are well suited to the resolution of such instruments. For nanostructures grown on Si and other conductive substrates SEM data at medium resolution (e.g. x 5,000) can be collected without the need for a sputtered Au layer, as the nanostructures tend to show intrinsic n-type conductivity in addition to the conductive substrates and charging effects are generally rather low. In the case of growth on insulating substrates such as sapphire and glass a sputtered Au layer is generally needed to reduce charging and enable reasonable image quality. In almost all cases when high resolution data is needed (e.g. > 100,000) a sputtered Au layer is required. A number of the figures earlier in the chapter (e.g. figure 2) show SEM images of various ZnO nanostructures, illustrating the capability of the technique for structural characterization, in plan view, cross-section and tilted views. SEM enables judgement of nanostructure array properties from uniformity, density and size dispersity down to the level of clear visualization of faceting on individual nanorods, shown in figure 12.

Another important method of structural characterization at the macrosopic scale (typically sampling areas of the order of mm^2) is x-ray diffraction (XRD). Again this is a very common technique, reported in many papers, see e.g. Cheng et al. (2005) and Kirkham et al. (2007), in order to determine the lattice constants of the ZnO nanorods. Depending on the degree of

texture and/or epitaxial relationship to the underlying substrate θ-2θ, ω and ϕ scan modes may all be used to elucidate the average crystal structure of the nanostructures, as described by Bauer et al. (1996). There appear to be 3 main "types" of ZnO nanorod samples as far as XRD is concerned: (a) randomly oriented growth (e.g. on Si substrates), (b) textured growth (e.g. on ZnO buffer layers on Si) and (c) epitaxial growth (e.g. on *a*-plane sapphire). In case (a) only θ-2θ data is required, as no structure would be expected in either ω or ϕ scan modes and a multiplicity of reflections is expected. The presence of multiple lines corresponding to various reflections from various ZnO planes is consistent with the random alignment of the nanstructures, i.e. a powder diffraction pattern is seen (or something very close to the powder pattern). This type of XRD pattern is often taken by itself as evidence of well-aligned nanostructures such as nanorods, and to a large extent this conclusion is sound, but it is worth pointing out that even in the case where only the {0001} ZnO reflections are seen in XRD, the nanostructures can still show a rather broad distribution of *c*-axis angles around the surface normal and this can only be quantified by a rocking curve measurement (ω scan). A very nice x-ray analysis of samples corresponding to cases (b) and (c) is reported by Cheng et al. (2005).

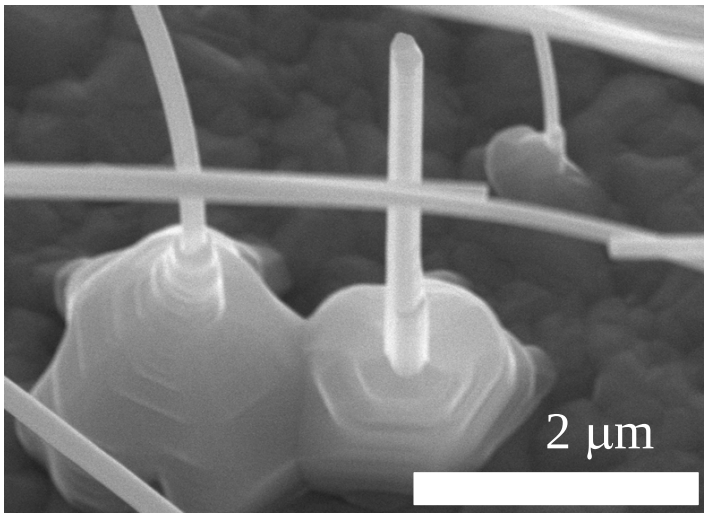

Fig. 12: SEM image of ZnO nanorods on a ZnO buffer layer on Si showing faceting on individual nanorods. Data courtesy of Dr. R.T. Rajendra Kumar.

TEM is among the most powerful microscopic structural characterization techniques available for the study of ZnO and other nanostructures as described by Reimer (1997). Clearly there is an associated cost in terms of the increased level of difficulty in sample preparation in certain cases. ZnO nanostructure samples can be prepared for TEM analysis in a variety of ways. If information concerning the relationship to the substrate is not required nanostructures can be removed from the substrate either by mechanical scraping or sonication, and then dispersed in a solvent and placed onto a TEM grid. If information concerning the relationship to the substrate is required then a more labour intensive route of sample preparation is generally required, including mechanical slicing (or cleaving), followed by further thinning using e.g. focused ion beam (FIB) methods. Depending on the substrate this can be a rather challenging process, and sapphire is a particularly difficult substrate requiring a rather extended sample preparation due to the material hardness. However, TEM provides unsurpassed resolution of nanostructure morphology and crystallography at a local level. Numerous examples exist in the literature of TEM studies (including lattice plane resolution using HR-TEM) of various types of ZnO nanostructure. Some examples are shown in figure

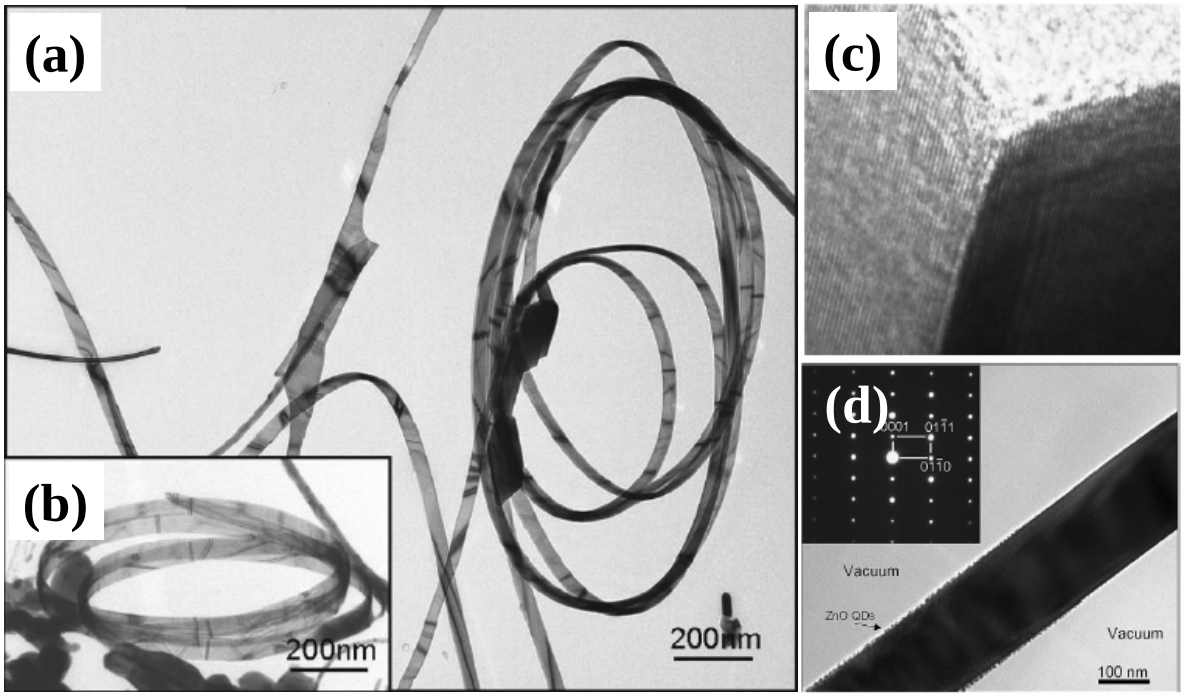

Fig. 13: Examples of TEM ((a) and (b)), HR-TEM (c) and SAED (d) data on various ZnO nanostructures. Images (a) and (b) reprinted with permission from Xiang Yang Kong, Applied Physics Letters, 84, 975 (2004). Copyright 2004, American Institute of Physics. Image (c) reprinted in part with permission from C. Borchers, J. Phys. Chem. B, 110, 1656 (2006). Copyright 2006, American Chemical Society. Image (d) reprinted with permission from Y. Ding, Surf. Sci., 601, 425 (2007). Copyright 2007, Elsevier Publishing.

13. In particular we note that TEM and selected area electron diffraction (SAED) studies from various groups have allowed very detailed studies to elucidate the structure of nanorods, nanowires, nanobelts and nanohelices e.g. as shown by Wang (2004), Kong et al. (2004a), Kong et al. (2004b) and Ding et al. (2007b). In addition, TEM AND HR-TEM has clarified the existence and nature of the epitaxial relationship of the Au nanodots found at the tips to the underlaying ZnO for VLS-grown ZnO nanorods; see e.g. Borchers et al. (2006). The majority of these studies indicate that individual nanostructures such as nanobelts, nanorods and nanowires (as opposed to structures which are clearly aggregates such as nanoflowers) are generally single crystalline, with relatively few examples showing consistent evidence of the presence of dislocations or other extended defects which might indicate a general pattern for nanostructure nucleation at such defects, as commented upon in section 3.1 earlier. This finding is consistent with the excellent optical and electrical properties of such nanostructures discussed in sections 4.2 and 4.3 below. One of the most active groups in the field (Z.L. Wang's group in the Georgia Institute of Technology and their co-workers) have made further interesting and important discoveries using painstaking TEM studies including the discovery of a cubic (zinc-blende) core for ZnO nanotetrapods, which clarifies the relationship of this commonly observed nanomorphology in ZnO to its "cousins" in other materials such as CdS and CdSe as reported by Ding et al. (2007a). In addition, SAED employing convergent

electron beams or other methods (as described by Ding et al. (2007b) and Wang et al. (2003)) offer the possibility of local determination of the polarity of {000x} surfaces in ZnO nanostructures (which is quite difficult to do using XRD because of Friedel's law, see e.g. Mariano et al. (1963) and references therein). This information can then be used to further understand secondary growth and related phenomena on those surfaces (e.g. catalytic behaviour) see e.g. Wang et al. (2003).

4.2 Optical characterization (including ensemble and single nanorod optical characterisation)

Some general aspects of the optical properties of ZnO have been discussed earlier and elements of the material properties relevant to optical emission have been summarized in section 2.4 above. It is fair to say that the majority of the impact of ZnO nanostructures on the optical properties of the system is due to the improvement in material quality attendant upon the excellent crystal quality often found in such systems, as mentioned earlier. However optical studies of ZnO nanostructures have also turned up many results whose explanation lies beyond effects simply associated with improved material quality.

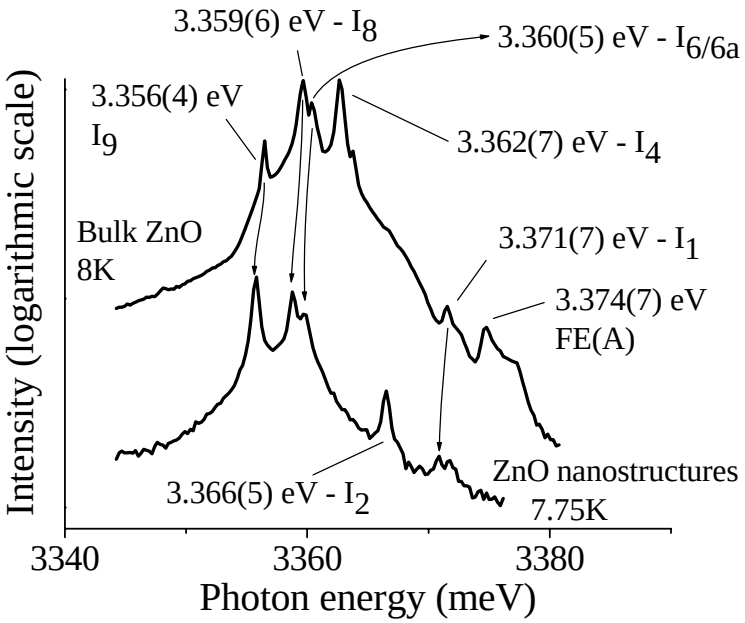

Fig. 14: Near bandedge PL from ZnO nanostructures on sapphire and comparison with PL from bulk ZnO. Data courtesy of Mr. Alan Meaney and Dr. J. Grabowska.

Interesting results have been obtained on the free exciton-polariton LO phonon coupling in nanowires of various sizes grown by different methods which indicate that surface effects may significantly influence this coupling and thus very strongly affect the room temperature position and linewidth of the UV bandedge emission (which is composed of overlapping bands from the free exciton and a number of its LO phonon replicas); see Voss et al. (2006). Additionally, the exciton-polariton mode in ZnO has also been discussed as a very suitable system in which to realize room temperature polariton lasers using a micro-cavity structure by Zamfirescu et al. (2002). The rather small value of the exciton Bohr radius for all excitons in ZnO (~ 2 nm) means that genuine exciton confinement effects including blueshifts of optical emission occur only in the very smallest dimension nanostructures and thin films; see Klingshirn (2007) and Makino et al. (2005). However, a number of relatively recent studies have also reported optical phenomena intrinsically associated with specific nanostructure morphologies. Very exciting

results on the confinement of exciton-polaritons in a ZnO nanowire and also the effects of whispering gallery modes in hexagonal ZnO nanowires on broad band defect emission have been published such as those by van Vught et al. (2006) and Nobis et al. (2004), both identifying intrinsic effects of nanostructure morphology on optical emission, beyond the effects of improved crystal quality and basic size dependent exciton confinement.

In addition, as commented upon in section 1, thin film and nanostructured ZnO samples (of crystal quality decidedly inferior to bulk single crystals in some cases) show optically pumped random lasing behaviour at room temperature, which has not been reported for single crystals. The origin of this enhancement for such samples compared to single crystals is still a topic of controversy and various hypotheses have been advanced. Data from our group has led to a proposal for the origin of this effect based on the inhibition of exciton diffusion in the small crystalline regions in thin films and nanostructures, leading to effective exciton trapping and anomalously high concentrations which favour the nonlinear emission bands in which random lasing is typically seen; see Tobin et al. (2006) and references therein.

Bandedge bound exciton emissions are seen regularly in low temperature PL studies of ZnO nanostructures, due to the excellent crystal quality of such material, and enable very detailed studies of such systems. An example is shown in figure 14 above of near bandedge PL from ZnO nanorods and nanowalls grown on sapphire. However, ZnO nanostructures also show additional bandedge PL features not seen (or seen only rarely or weakly) in bulk material of comparable quality, attributed to the high surface to volume ratio of such morphologies. One recent example is the so-called “surface exciton” emission at ~ 3.3665 eV reported by Grabowska et al. (2005). Low temperature studies from the early 1990s identified a high energy line at ~ 368.2 nm (3.367(4) eV) as due to recombination of a surface-related exciton in ZnO, observed in luminescence studies of a range of samples incorporating ZnO crystallites with a high surface to volume ratio, possibly due to an exciton bound at a surface adsorbed oxygen atom or molecule; see Grabowska et al. (2005), Savikhin et al. (1993) and Travnikov et al. (1990). Recent work from our group and others (Wischmeier et al. (2006a)) has strengthened this assignment. Figure 14 also shows a comparison between low temperature PL spectra from bulk crystal material and ZnO nanostructured material. We see no evidence for the surface-related exciton at 3.3665(1) eV from the bulk crystal sample, although it shows luminescence from various members of the I-line series.

Various authors have reported correlations between the green to UV emission intensity ratios and nanoparticle or nanostructure dimension, and have interpreted these data in terms of surface effects due to the changing surface to volume ratios of nanostructured morphologies, including the effects of oxygen deficient surfaces, band bending and depletion region formation which changes the defect charge state and its emission as reported by Vanheusden et al. (1996) and Shalish et al. (2004).

Finally, more recent studies such as those of Wischmeier et al. (2006b) have concentrated on the differences in optical properties of ensembles of nanowires compared to single nanowire properties using cathodoluminescence (CL), PL and micro-PL spectroscopies. These studies have been very important in showing that, amongst other results, the emission

of typical single nanorods correspond rather closely in most cases to the emission from an ensemble of excited nanowires, which raises confidence that large area excitation and collection PL measurements reflect the average PL properties of the nanowires faithfully and that the spread in such properties is not so large as to render the large area PL data useless for interpretation of nanowire properties.

4.3 Electrical characterization (including ensemble and single nanorod electrical characterisation)

A number of reports have examined the electrical properties of ZnO nanostructures. Amongst other goals, some of these have had the aim of exploiting the high crystalline quality of these structures in the expectation of positive outcomes for electrical properties such as a reduced n-type background to overcome in order to achieve type inversion. However, electrical characterization of ZnO nanorods in general has been carried out rather less extensively than the common optical and structural characterization methods, due at least in part to the additional difficulties and processing steps associated in contacting arrays of nanorods and single nanorods. A detailed discussion of issues pertaining to contacting of ZnO is given by Ozgur et al. (2005) and Heo et al. (2004a).

A number of the older reports on the electrical response and properties of ZnO nanorods have studied the properties of ensembles of nanorods, both aligned and unaligned. In many cases these studies have been based around the use of nanorod ensembles as devices of one sort or another such as sensors, p-n junctions, etc., as reported by Heo et al. (2004a) and Willander et al. (2008a), and a more detailed discussion of such applications will follow in section 5.3. However, more recently reports have appeared on the electrical properties of single ZnO nanorods and nanowires, which are grown in ensembles and then dispersed on e.g. Si substrates and contacted using various lithographic techniques. The contacting has been made in a number of ways to allow both ohmic and Schottky diode behaviour to be studied in single nanorod systems; see Heo et al. (2004a). The Si substrate can also be used as a back gate to form a single nanowire FET structure; see e.g. Hong et al. (2008a), (2008b) and Cao et al. (2008). The results of these studies generally indicate that nominally undoped ZnO nanowires show an appreciable background n-type carrier concentration in the range 10^{16} cm^{-3} – 10^{18} cm^{-3}, very similar to the ranges found in bulk and thin film samples; see e.g. Heo et al. (2004b) and Hong et al. (2008a). However, the mobility values in many cases are appreciable larger than those obtainable in most thin films, in the range 20 – 150 cm^2/Vs at room temperature (see e.g. Hong et al. (2008b)), which is comparable to the single crystal mobility at room temperature (> 100 cm^2/Vs, see e.g. Klingshirn (2007)). These rather high mobility values are in line with the known crystalline quality of nanorods, and indeed they are quite high considering the likelihood of carrier scattering at nanostructure walls. The other important outcome of a number of electrical transport studies on ZnO nanostructures is that the carrier concentrations and mobilities are strongly affected by the environment of the nanostructures (including gas ambient and illumination conditions) and these quantities can be controlled and improved by the use of e.g. passivating layers as discussed by Heo et al. (2004a) and Hong et al. (2008b). This sensitivity of ZnO properties to the environment is a long established aspect of the material and the physical chemistry of ZnO surface interactions

such as molecular adsorption and chemisorption are well known, as are their effects on photoconductivity and surface band bending described by Hirschwald (1985). It is thus not very surprising that these effects will have an impact on ZnO nanostructure properties given the large surface to volume ratio of these structures and the proportionately larger surface area presented. This aspect of the electrical behaviour of ZnO nanowires is likely to pose challenges for some applications where electrical stability in the long term is an important or desirable quality (such as optoelectronic emitters) but may also yield many applications in terms of sensing.

5. ZNO NANOSTRUCTURE APPLICATIONS

5.1 Electrical, optical/photonic applications

One of the main application areas in which ZnO nanostructures are hoped to make an impact is in optoelectronic and photonic devices such as LEDs and LDs. The excellent crystalline quality is expected to lead to efficient excitonic emission up to room temperature and various devices such as polariton lasers have been discussed as technological possibilities based on ZnO. However, the same bottleneck of p-type doping affects nanostructures as has affected bulk and thin film materials for many years. While excellent optical properties and other behaviour is observed in ZnO nanostructures under e.g. optical or electron beam excitation, it has not been possible to electrically pump optoelectronic devices made solely from ZnO (i.e. homojunction devices).

In order to overcome this barrier, a number of groups have attempted novel p-n junction device structures. Koenenkamp et al. (2004) and Park et al. (2004) report the fabrication of vertically aligned ZnO nanowire- or nanorod-based light emitting devices. In both cases these were heterostructure devices where hole injection was from another p-type material, in one case using a p-type polymer (Koenenkamp et al. (2004)) and in the other p-GaN (Park et al. (2004)). The devices utilize ensembles of reasonably well-aligned ZnO nanorods. The gaps between individual nanorods are filled by insulating polymers in both cases. The p-type layers then connect either to the nanorods tips (in the case of the p-type polymer) or at the nanorod bases (p-GaN). A broadly similar structure has been reported by Willander et al. (2008b) using polymer electron blocking layers in addition to p-type polymers to encourage hole injection into ZnO as the main current transport mode across the junction. In all these cases current rectification is seen. In the case of the ZnO nanorod / p-GaN structure broad band electroluminescence is seen with both visible and UV emission which is attributed to both ZnO and GaN contributions (Park et al. (2004)). For the ZnO nanorod / p-polymer structure once again a broad electroluminescence band is seen (Park et al. (2004)). Another ZnO nanowire based light emitting device is reported by Bao et al. (2006) using a single ZnO nanowire dispersed on a p-type silicon substrate (as a hole injector) and coated with an insulating polymer. Selective etching of this insulating polymer is performed using e-beam lithography and finally metal electrodes were deposited. This device utilises the large surface area associated with the nanowire for carrier injection (p-n junction formation) compared with the device described by Koenenkamp et al. (2004). Once again current rectification behaviour

and broad band visible electroluminescence were observed.

The experiences of groups using such heterostructures for p-n junction formation seems to parallel those of the thin film community. In most cases current rectification and electroluminescence is observed from these structures, often with a broad band emission. Rogers et al. (2006) have seen UV electroluminescence emission (375 nm) without any apparent visible emission from a n-ZnO/p-GaN heterostructure, but the emission intensities appear to be quite weak even at the highest currents. The reports of Tsukazaki et al. (2005) on a ZnO p-n homojunction using the repeated temperature modulation growth technique also show a broad band electroluminescence emission.

Despite the inventive device design strategies used, it appears that the performance of ZnO nanostructure light emitters remains far from optimized, given the potential of such nanostructures for strong UV and visible emission. The difficulties in hole injection associated with the absence of p-type ZnO have not yet been overcome by the use of heterostructure devices. Issues concerning band offsets remain to be solved for both p-type Si and p-type polymers, while the relative advantages of using p-GaN/n-ZnO compared to GaN devices are not clear. Furthermore, the broad band emission, while potentially useful for lighting applications if it can be reproducibly controlled by defect engineering, is not the strong UV source hoped for and will certainly not suffice for applications such as high density optical storage and retrieval. In addition, the potential advantages of the large surface to volume ratio of ZnO nanowires have not been utilized in heterostructure ensemble devices. By contrast, the single nanorod device discussed by Bao et al. (2006) does utilize this geometric advantage, but it is unlikely that the processing needed for such single nanostructure devices will be readily adaptable for mass production with current technology since it is difficult to assemble an array of nanowires in the ordered fashion suitable for processing.

Hence, despite the materials promise of ZnO and ZnO nanostructures in particular, the difficulties presented by the p-type doping issue remain to be solved and appear to be as big an obstacle for ZnO nanostructures as they have proven for thin films.

5.2 Field emission applications

Despite the difficulties in the utilization of ZnO nanostructures in p-n junction devices, the self-organised nanomorphologies still offer a great deal of promise for device structures not requiring bi-polar doping. One such application area is field emission, which is a quantum-mechanical effect whereby free electrons from a metal or a semiconductor can tunnel into a vacuum in the presence of an electric field applied on the surface, but in the absence of any heating as described by Silva et al. (2005). Field emission is also known as cold cathode emission and has tremendous potential in applications where small, intense, sources of electrons are needed such as flat panel displays, miniature x-ray sources or microelectronics. In particular, as cathode ray tube (CRT) technology is progressively being abandoned by numbers of television and portable computer manufacturers and the market for flat panel displays (FPD) is expanding very fast. One can also mention the recent commercial

availability of flexible and portable “electronic” sheets that will soon compete with the printed paper media (see e.g. http://www.plasticlogic.com). In addition, the possibility of using such electron sources for more general lighting applications in conjunction with phosphors is an attractive possibility for new energy-efficient lighting solutions. Liquid Crystal Display (LCD) technology is currently the dominant FPD technology, but other ones such as plasma, organic-polymer and field-emission displays are also rapidly emerging. There are intrinsic difficulties such as inferior resolution and the use of expensive thin film transistor (TFT) addressing schemes which make scale-up of LCD technology quire difficult. These other display technologies therefore may all find eventual uses in certain markets because the type of information to be displayed will influence the choice of display type. For this reason there is a strong need to carry out research in these areas.

Carbon-based materials such as hydrogenated amorphous carbon (a-C:H) and carbon nanotubes (CNT’s) have been intensively researched in the last decade as they are considered excellent field emission electron source candidates due to their low electron affinity and advantageous shape, ie a high aspect ratio which is known to favour field emission by increasing the field enhancement factor discussed by Amaratunga et al. (1996) and Bonnard et al. (2001). However, commercial development has been hindered due to the poor emission uniformity that seems to be invariably obtained with these materials, the origin of which probably rests with a lack of reproducible uniformity in the large area growth of these structures; see Silva et al. (2005). As a result research into alternative materials to CNT’s for the production of FE electron sources has begun with materials that readily form wire-like structures, have attractive electronic properties and high thermal stability being the prefered choices. Clearly one such material is ZnO, which makes it a natural candidate. ZnO nanowire-like structures have recently demonstrated interesting field emission properties, as reported by Lee et al. (2006) and Yang et al. (2006), with typical maximum emission current density of 1 mA/cm^2 at a threshold field of about 8.0V/μm. Various reports have indicated that ZnO nanostructures of various morphologies can be used as effective field emitters, and improvements in performance based on surface modifications such as coating with amorphous carbon and carbon nitride have been recently achieved; see Liao et al. (2005). The natural nanostructured morphology means that significant field enhancement factors (β) may be expected based on aspect ratio considerations alone. An example of field emission data (from our group and that of J.D. Carey in the University of Surrey, UK) using arrays of ZnO nanorods grown on ZnO thin film buffer layers on (001) Si is shown in figure 15; see Rajendra Kumar et al. (2007b).

A number of studies show that typical field enhancement factors of ~ 1000 are observed even for nanostructures such as nanorods (using a work function value of 5.2 eV for the electrons in ZnO below the vacuum level) where the aspect ratios based solely on the nanostructure geometry are expected to be an order of magnitude smaller; see Rajendra Kumar et al. (2007b)). These results imply that in many cases the field enhancement is due not only to the aspect ratio of the structures but also to the very sharp edges and points associated with the faceting seen in ZnO nanowires grown by certain techniques which give field enhancement factors generally larger than the aspect ratios of the geometry alone would suggest.

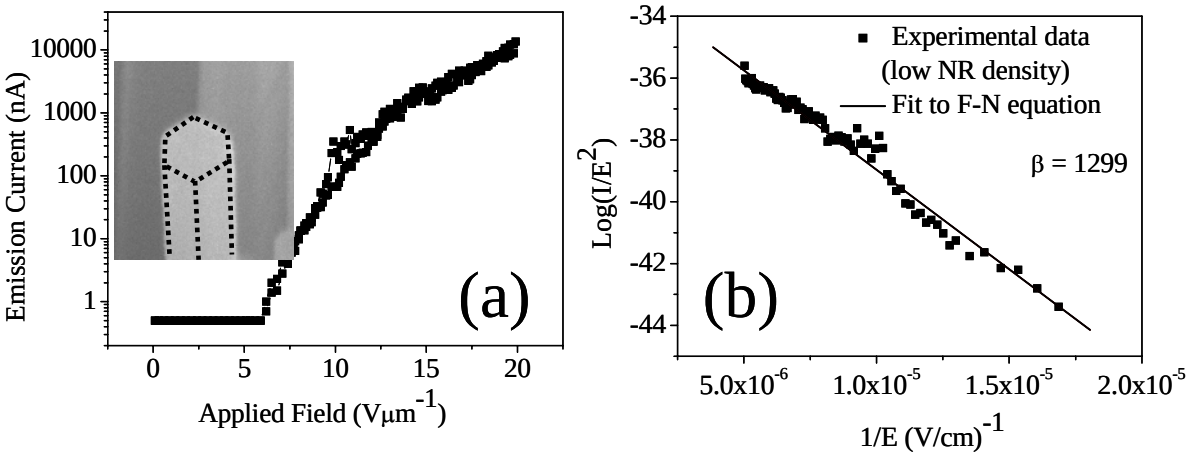

Fig. 15: (a) FE current as a function of applied field from ZnO nanorods. Inset shows SEM image of sharp facet edges (highlighted by dashed lines) of a typical nanorod, (b) Fit to Fowler–Nordheim equation with fitted field enhancement parameter, β, shown. Images reused with permission from R.T. Rajendra Kumar, Nanotechnology, 18, 215704 (2007). Copyright 2007, Institute of Physics.

The main issue affecting the utilisation of ZnO nanowires at a commercial level for field emission applications is that of nanostructure placement and spacing. Only by controlling the aspect ratio, faceting and spacing can the field enhancement factor be enhanced while the effects of shielding (screening) due to nearby nanostructures are reduced to yield an optimized field emission with uniform performance over a large area substrate. Control of these parameters is a major challenge in ZnO nanoscience. Recent work from our group (Rajendra Kumar et al. (2007b)) has shown that parameters such as furnace ramp rate in self-organised VPT growth can be utilized to control nanorod spacing and thus improve field emission uniformity, but further work is ongoing to build upon these initial results.

However ZnO nanostructures offer unique possibilities for the construction of field emission devices. The thermal, chemical and structural stability of the material combined with the high field enhancement factors nanostructures naturally offer means that devices based on ZnO may prove superior to carbon-based technologies in many respects.

5.3 Applications in sensing, energy production, photochemistry, biology and engineering

In addition to the ZnO applications discussed above in sections 5.1, 5.2 and also more broadly in section 1 a number of other promising application areas for ZnO nanostructures have been reported recently in a diverse range of technological spaces and in this section we will very briefly summarise them.

The use of ZnO nanostructures for sensing applications has been an ongoing activity for a rather long period of time. A number of reports exist on sensing of various gaseous species, including hydrogen, ozone and ethanol; see e.g. Liu et al. (2005), Wang et al. (2005) and

Kang et al. (2005). A comprehensive review of this area has been published recently by Willander et al. (2008). These reports generally measure the conductivity of ZnO nanostructures in various gas ambients as a sensing strategy. The adsorption and chemisorption of different gases onto ZnO alters the carrier density in the structures and thus their electrical conductivity, providing a convenient measureand; see Wang et al. (2005). The surface activity of ZnO has been commented upon earlier in relation to electrical measurements in section 4.3 and mainly described as a negative aspect in terms of stability of electrical properties of the material. However, as in many areas of ZnO research, certain material properties when viewed from one perspective may be seen as disadvantages whereas when viewed from other perspectives, and with different applications in mind, may be seen as key material advantages. The high surface to volume ratio of ZnO nanostructures makes sensing applications a natural area of research. Furthermore, the crystallographically facetted nature of ZnO nanostructures grown by a number of techniques and reports of signficant adsorption and chemisorption of gases on these facets with substantial differences in behavour on different facets (e.g. Gay et al. (1980)), means that ZnO nanorods offer not only the possibility of highly sensitive gas sensing but also selective sensing of various gas species via control of nanostructure morphology. The combination of both these features means that ZnO has exceptional potential for gas sensing applications.

One of the most exciting applications for ZnO nanostructures reported recently has been their use for electrical energy generation, using the intrinsic piezo-electric property of the ZnO crystal referred to in section 2.5, by the Wang group at the Georgia Institute of Technology;

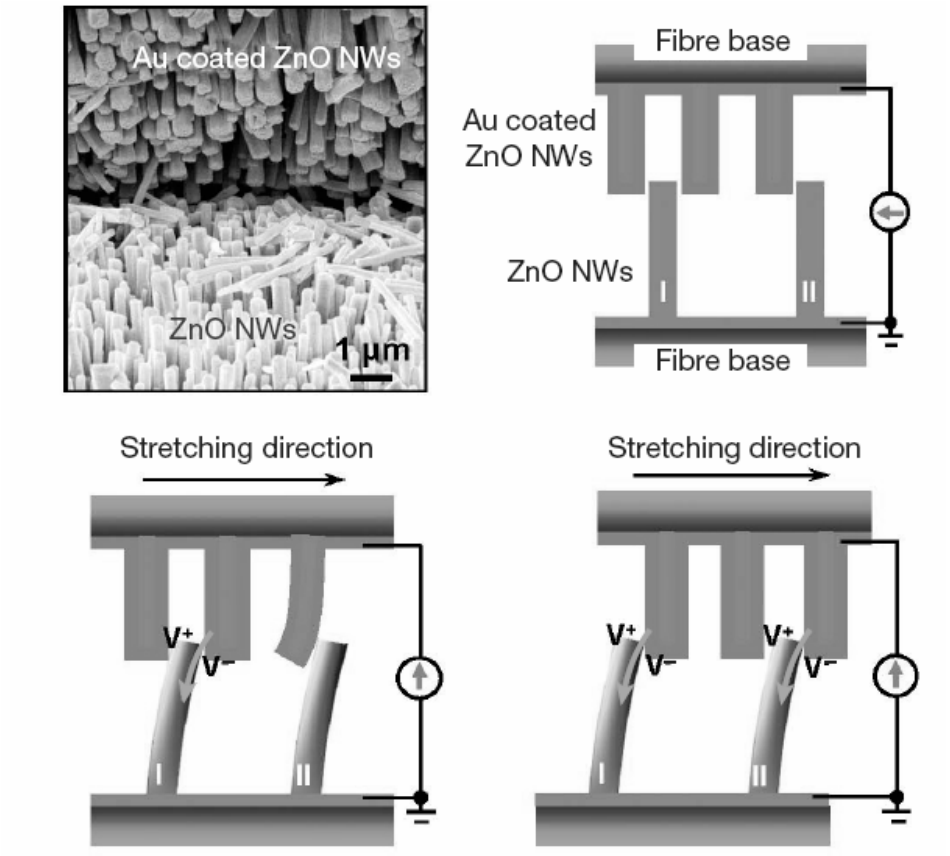

Fig. 16: Schematic diagram of ZnO nanopiezotronic circuit. Image reprinted by permission from Macmillan Publishers Ltd: Nature; Y. Qin, Nature, 451, 809 (2008). Copyright 2008.

see e.g. Wang (2007), Qin et al. (2008). A schematic diagram of the process is shown in figure 16. The process relies on the use of arrays of aligned ZnO nanorods. When these nanorods are strained under shear, a piezo-electric voltage is developed across the nanorods. By contacting the tips of these nanorods using e.g. a Schottky metal contact such as a Pt scanning probe microscope tip or another (Au-coated) nanorod array, a rectifying circuit can be formed allowing a current to flow and electrical power to be extracted from the strain energy of the nanorods. Among the applications envisaged for such structures is the harnessing of "parasitic" energy (such as biological mechanical energy and acoustical energy) for electrical power. Devices operating on this principle could be installed in e.g. the soles of shoes, to harness the periodic strain associated with walking motion to create electrical power, which might be stored and/or used to operate a range of personal electrical or electronic devices. Z.L. Wang (2007) has coined the term "Nanopiezotronics" to describe these and related applications in e.g. sensing and resonators. Certainly these applications are likely to be of very great interest in the near future given the increasing social and environmental requirements for new energy sources and innovative use of many small energy sources rather than relying on fossil fuels. The material requirements for wide scale use of this technology do not appear unduly reliant on very high crystalline quality, and seems rather more focused on the ability to form uniform nanostructure arrays with suitable morphologies over large areas on various (probably flexible) substrates.

Finally, we also wish to note that a number of very interesting application areas involving ZnO at the interface with photochemistry, biology and engineering have also been reported. The chemical modification of materials such as TiO_2 using e.g. ruthenium- or osmium-based chemical dye compounds for applications involving photochemically-induced charge transfer in e.g. Graetzel cells have been known for many years; see the review by Kamat (2007). The broadly similar electronic properties of ZnO nanostructures to TiO_2 (at least in regard to electron injection between the semiconductor and the dyes) has led a number of groups to attempt to modify ZnO nanostructures with chemical dyes in an analagous fashion for similar applications; see e.g. Law et al. (2005) and Groarke et al. (2005). The ability to grow ZnO nanostructures with very high surface to volume ratios promises a very high interface area between the ZnO and the dye molecules which may lead to rather high quantum efficiency for Graetzel cells based on these structures. Photovoltaic cells based on ZnO-based structures have been reported with efficiencies of ~ 1.5 %, but this is much lower than that of devices using chemically modified TiO_2 nanocrystalline thin films (~ 10 %). It appears that while many aspects of bandstructures such as band offsets are similar in the case of TiO_2 and ZnO, some key aspects of the photo-chemical charge transfer process including key lifetimes are much poorer for these applications in the case of ZnO, and the prospects for this technology based on ZnO does not appear very bright at present; see e.g. Furube et al. (2006). The interface of ZnO nanostructures with biological species is also an interesting area of research. It has been noted in section 1 that ZnO is already used for a range of bio-applications including e.g. fungicides, cosmetics and pharmaceuticals. The use of ZnO nanorods and other nanostructures in other bio-applications has also been reported recently including applications as a textured substrate for cell growth by Grabowska et al. (2007), as part of a sensor system for high sensitivity detection of fragments of bio-molecules such as protein and DNA sequence detection by Kumar et al. (2006), for photocatalytic inactivation of pathogenic

biofilms by Mosnier et al. (2006) and for intracellular pH measurements using ZnO nanowires by Al-Hilli et al. (2007). These bio-applications represent a very exciting synergy between inorganic semiconductor nanoscience and biology/biotechnology. Engineering applications of ZnO nanostructures include the use of arrays of well-aligned ZnO nanorods as superhydrophobic or tunable surfaces (whose properties are controllable between superhydrophobic and superhydrophillic via exposure to UV radiation) for e.g. fluid flow and heat transfer control in microfluidic systems as reported by Li et al. (2005) and Feng et al. (2004). These applications are similar to those involving TiO_2 films reported by Karuppuchamy et al. (2005). The naturally low contact area of ZnO nanostructures makes the contact angle for these surfaces high (i.e the surfaces are hydrophobic). Exposure to UV radiation leads to the generation of electron-hole pairs close to the surface which interact with adsorbed surface species and alter the nature of the surface, changing it to a superhydrophillic surface (i.e. almost zero contact angle).

6. CONCLUSIONS AND ACKNOWLEDGMENTS

In the preceding sections, we have tried to give a brief overview and flavour of the many exciting activities currently in progress in the ZnO nanostructure research community. Given this breadth of activity and its continuing growth, it appears useful for the authors to hazard some guesses as to where ZnO nanostructures are likely to make significant technological contributions (if only so that we can look back to see how wrong we actually were).

Applications of ZnO nanostructures in electronic and photonic devices such as LEDs and LDs are very exciting given the material quality of the nanostructures. However, the lack of reliable p-type doping remains a huge impediment to any advances in this area. Alternative device strategies seem to either suffer from rather large technical difficulties in terms of band offsets or to offer little advantages over e.g. GaN technology. Furthermore, the nanostructured morphology in many cases is not used to best advantage, and single nanowire devices are unlikely to be mass producible. Thus while the potential of this field is very high, the challenges to be met are considerable.

It seems to us that application of ZnO nanostructures in areas where bipolar structures are not required offer just as many materials advantages without such significant problems. In this regard the use of ZnO nanostructures as field emission sources for e.g. FPDs and energy efficient lighting is a most promising application area. Similarly the applications in sensing, energy production, photochemistry, biology and engineering discussed in the preceding section all benefit to a greater or lesser extent from ZnO materials properties and/or its naturally nanostructured morphology, without very significant technological barriers. Among these the use of ZnO nanostructures for parasitic power generation using its piezo-electric property is a very exciting new area and may have significant impact as part of a global shift in patterns of power generation, storage and consumption.

The use of ZnO nanostructures in devices on the industrial scale will require significant improvements in our ability to synthesise specific morphologies with reasonable yield over

large area substrates. As mentioned in sections 1 and 3.1 earlier, the absence of detailed understanding of the growth mechanism in many cases makes this a difficult challenge. Certain growth techniques seem better suited to achieving this goal than others. MOCVD for example seems to show rather better reproducibility of growth than VPT techniques generally and is ideally suited to large area substrates, particularly when compared to methods such as PLD where large area growth is a significant challenge. In addition MOCVD is already a recognized and developed tool in the semiconductor industry and thus will be more likely to gain the acceptance of manufacturers considering new devices and materials (as a known and trusted quantity). CS growth will certainly also be an attractive prospect for manufacturers in many ways, particularly in terms of cost, potential for large area coverage, range of possible substrates useable (including flexible, plastic substrates) and the low processing temperatures required. For applications where specific morphologies rather than very high crystal quality are required (e.g. field emission and perhaps also sensing, piezo-electric power generation and bio-applications) CS growth may be ideal.

However, among the most serious threats to ZnO work over the next 5 years will be that the focus, of both researchers and funding agencies, will drift away to newer or greener scientific pastures. We mentioned in section 1 that the loss of interest in ZnO in the period 1970 – 1990 was due in part to severe difficulties in doping the material both n- and p-type combined with rapid advances in new physics associated with III-V low dimensional structures. The same threat exists now as the p-type doping problem remains unsolved to the extent long hoped for, despite the huge effort in this direction. This problem is compounded by the fact that a great deal of funding worldwide has been given to ZnO research (often for research on p-type doping) and the natural (and legitimate) expectation of the funding agencies is that device applications will result from this funding. If this does not prove to be the case, these agencies will quickly turn their attention elsewhere. It is important therefore that the many materials advantages and unique morphologies which ZnO nanostructures can offer remain on the “radar screen” of science funding agencies, through continuing research efforts on a broad front in this area and hopefully the realization of practical devices, perhaps in the p-n junction / optoelectronic domain but equally importantly in areas such as field emission, sensing etc. which are in many ways ripe for short to medium term exploitation.

We would like to acknowledge both the many contributions of our colleagues in ZnO research over the past 10 years to our own understanding and appreciation of the field. We have been fortunate to work with a range of talented postdoctoral fellows in Dublin City University (DCU) including Drs. Chaitali Roy[+], Karuna Kar Nanda, J.R. DuClere, R.T. Rajendra Kumar and B. Doggett. In addition we have been fortunate to have had such talented postgraduate students in our groups working on ZnO, including Dr. Justyna Grabowska, Mr. Ricky O’Haire, Mr. Alan Meaney, Mr. Conor McLoughlin and Ms. Sarah Byrne. We have benefited very much from the opportunity to speak with such ZnO luminaries as Prof. Dr. Claus Klingshirn (University of Karlsruhe, Germany) and Prof. David Look (Wright State University, USA) and the opening section of the current chapter has been informed in many aspects by a number of previous reviews of various aspects of ZnO materials and thin films written by these authors. We also ackowledge the many contributions of other colleagues around the world, including Dr. S. Newcomb of Glebe Laboratories, Tipperary, Ireland for his

collaboration with us providing TEM studies of ZnO and other nanostructures, Dr. J.D. Carey in the University of Surrey, UK, on field emission work and also those many colleagues involved in the EU FP6 Thematic Network “SOXESS”.

Finally, our work on ZnO would not have been possible without significant financial support from a range of sources and it is a pleasure for us to acknowledge grant funding from Science Foundaation Ireland (SFI, under their PI, RFP, UREKA, STARS and equipment supplement programmes), Enterprise Ireland (under their Basic Research grant programme), the Irish Higher Education Authority (HEA, under their PRTLI programme, cycles I and IV, as part of the National Development Plan), the European Union (EU, through the FP6 Thematic Network “SOXESS”) and various sources of internal funding from. DCU through the School of Physical Sciences, the National Centre for Plasma Science & Technology (NCPST) and various other university-wide schemes.

[+]Dr. Chaitali Roy was a former postdoctoral researcher in the authors' group involved in the initial phases of ZnO research in the School of Physical Sciences and National Centre for Plasma Science & Technology at Dublin City University. Dr. Roy was a native of West Bengal, India and completed her M.Sc. in Physics at Utkal University, Orissa, India in 1991, and her Ph.D. on Raman spectroscopic studies of Lanthanum-Barium Manganites at the Indian Institute of Technology, Kanpur, India in the year 2000. Dr. Roy passed away in Kolkata, India on 21 May 2005 after a long illness, aged 36. We dedicate this chapter to her memory, in gratitude for her many scientific and personal contributions to our group.

REFERENCES

Al-Hilli, S.M., Willander, M., Ost, A. and Stralfors, P. (2007) J. Appl. Phys. 102 084304.

Almamun Ashrafi, A.B.M., Ueta, A., Avramescu, A., Kumano, H., Suemune, I., Ok, Y.-W. and Seong, T.Y. (2000) Appl. Phys. Lett. 76 550.

Amaratunga, G. and Silva, S.R.P. (1996) Appl. Phys. Lett. 68 2529.

Ameta, S.C., Chaudhary, R., Ameta, R. and Vardia, J. (2003) J. Ind. Chem. Soc. 80 257.

Bagnall, D.M., Chen, Y.F., Shen, M.Y., Zhu, Z., Goto, T. and Yao, T. (1998) J. Crys. Growth 184-185 605.

Barnard, A.S., Xiao, Y. and Cai, Z. (2006) Chem. Phys. Lett.

Bateman, T.B. (1962) J. Appl. Phys. 33 3309.

Bates, C.H., White, W.B. and Roy, R. (1962) Science 137 993.

Bai, W., Yu, K., Zhang, Q.X., Zhu, X., Peng, D.Y., Zhu, Z.Q., Dai, N. and Sun, Y. (2008) Physica E 40 822.

Bao J., Zimmler, M.A., Capasso, F., Wang, X.W. and Ren, Z. F. (2006) Nano Lett. 6 1719.

Bauer, G. and Richter, W. (1996) *Optical Characterisation of Semiconductor Layers*, Springer-Verlag, Berlin and Heidelberg.

Bekeny, C., Voss, T., Gafsi, H., Gutowski, J., Postels, B., Kreye, M. and Waag, A. (2006) J. Appl. Phys. 100 104317.

Berg, W.F. (1938) Proc. Roy. Soc. A 164 79.

Blattner, G, Kurtze, G., Schmeider, G. and Klingshirn, C. (1982) Phys. Rev. B 25 7413.

Bonnard, J.M., Kind, H., Stockli, T. and Nilsson, L.O. (2001) Solid State Electron. 45 893.

Borchers, C., Mueller, S., Stichtenroth, D., Schwen, D. And Ronning, C. (2006) J. Phys. Chem. B 110 1656.

Börrnert, F., Lavrov, E.V. and Weber, J. (2007) Phys. Rev. B 75, 205202.

Brown, M.E. (1957) *ZnO – Rediscovered*, The New Jersey Zinc Company, New York.

Bragg, W.L. (1920) Phil. Mag. 39 647.

Bunn, C.W. (1935) Proc. Phys. Soc. 47 835.

Cao, B.Q., Lorenz, M., Brandt, M., von Wenckstern, H., Lenzner, J., Biehne, G. and Grundmann, M. (2008) Phys. Stat. Sol. RRL 2 37.

Casella, R.C. (1959) Phys. Rev. 114 1514.

Chambers. A., Fitch, R.K. and Halliday, B.S. (1998) *Basic Vacuum Technology*, IOP Publishing, Bristol, UK.

Cheng, H.M., Hsu, H.C., Yang, S., Wu, C.Y., Lee, Y.C., Lin L.J. and Hsieh, W.F. (2005) Nanotechnology 16 2882.

Claeyssens, F., Freeman, C.L., Allan, N.L., Sun, Y., Ashfold, M.N.R. and Harding, J.H. (2005) J. Mater. Chem. 15 139.

Claflin, B., Look, D.C. and Norton, D.R. (2007) J. Elec. Mat. 36 442.

Crisler, D.F., Cupal, J.J. and Moore, A.R. (1968) Proc. IEEE 56 225.

Czekalla, C., Guinard, J., Hanisch, C., Cao, B.Q., Kaidashev, E.M., Boukos, N.., Travlos, A., Renard, J., Gayral, B., Le Si Dang, D., Lorenz, M. and Grundmann, M. (2008) Nanotechnology 19 115202.

Ding, Y., Wang, Z.L., Sun, T.J. and Qiu, J.S. (2007a) Appl. Phys. Lett. 90 153510.

Ding, Y. and Wang, Z.L. (2007b) Surf. Sci. 601 425.

Dingle, R (1969) Phys. Rev. Lett. 23 579.

Djurisic, A.B. and Leung, Y.H. (2006) Small 2 944.
Elliott, R.J. (1957) Phys. Rev. 108 1384.
Fan, H.J., Lee, W., Hauschild, R., Alexe, M., Le Rhun, G., Scholz, R., Dadgar, A., Nielsch, K., Kalt, H., Krost, A., Zacharias, M. And Goesele, U. (2006) Small 2 561.
Fan, H.J., Barnard, A.S. and Zacharias, M. (2007) Appl. Phys. Lett. 90 143116.
Fang. X., Bando, Y., Gautam, U.K., Ye, C. and Golberg, D. (2008) J. Mat. Chem. 18 509.
Feng, X.J., Feng, L., Jin, M.H., Zhai, J., Jiang, L. and Zhu, D.B. (2004) J. Am. Chem. Soc. 126 62.
Fiebig, M., Froehlich, D. and Pahlke-Lerch, Ch. (1993) Phys. Stat. Sol. (b) 177 187.
Forty, A.J. (1952) Phil. Mag, 344 949.
Fowler, R.H. and Nordheim, L. (1928) Proc. Roy. Soc. A 119 173.
Freeman, C.L., Claeyssens, F., Allan, N.L. and Harding, J.H. (2006) Phys. Rev. Lett. 96 066102.
Fuller M.L. (1944) J. Appl. Phys. 15 164.
Furube, A., Murai, M., Watanabe, S., Hara, K., Katoh, R. and Tachiya, M. (2006) J. Photochem. Photobiol. A: Chemistry 182 273.
Gay, R.R., Nodine, M.H., Henrich, V.E., Zeiger, H.J. and Solomon, E.I. (1980) J. Am. Chem. Soc. 102 6752.
Gil, B. (2001) Phys. Rev. B 64 201310.
Goniakowski, J., Noguera, C. and Giordano, L. (2004) Phys. Rev. Lett. 93 215702.
Grabowska J., Meaney, A., Nanda, K.K., Mosnier, J.-P., Henry, M.O., Duclère, J.-R. and McGlynn, E. (2005) Phys. Rev. B 71 115439.
Grabowska, J., O'Sullivan, F., Clynes, M. and McGlynn, E. (2007) Workshop on Plasma Processes for Biomedical Applications, May 24th 2007, NCPST, DCU, Dublin, Ireland.
Greene, L.E., Law, M., Tan, D.H., Montano, M., Goldberger, J., Somorjai, G. and Yang, P. (2005) Nano Lett. 5 1231.
Greene, L.E., Yuhas, B.D., Law, M., Zitoun, D. and Yang , P.D. (2006) Inorg. Chem. 45 7535.
Groarke, R., Grabowska, J., Nanda, K.K., McGlynn, E. and Vos, J.G. (2005) Proc. SPIE 5826 194.
Gutowski, J., Baume, P. and Hauke, K. (1997) *Properties of Wide Gap II-VI Semiconductors*, (Ed. Bhargava, R.) INSPEC, London.
Halsted, R.E. and Aven, M. (1965) Phys. Rev. Lett. 14 64.
Huang, Y., Yu, K. and Zhu, Z.Q. (2007) Curr. Appl. Phys. 7 702.
Hauschild, R., Priller, H., Decker, M., Kalt, H. and Klingshirn, C. (2006a) Phys. Stat. Sol. (c) 3 980.
Hauschild, R., Priller, H., Decker, M., Brueckner, J., Kalt, H. and Klingshirn, C. (2006b) Phys. Stat. Sol. (c) 3 976.
Heiland, G., Mollwo, E. and Stockmann, F. (1959) Sol. State Phys. 8 191.
Heitz, R., Hoffmann, A. and Broser, I. (1992) Phys. Rev. B 45 8977.
Heo, Y.W., Norton, D.P., Tien, L.C., Kwon, Y., Kang, B.S., Ren, F., Pearton, S.J. and LaRoche, J.R. (2004a) Materials Science and Engineering R 47 1.
Heo, Y.W., Tien, L.C., Kwon, Y., Norton, D.P., Pearton, S.J., Kang, B.S. and Ren, F. (2004b) Appl. Phys. Lett. 85 2274.

Hirschwald, W.H. (1985) Acc. Chem. Res. 18 228.
Hong, W.K., Sohn, J.I., Hwang, D.K., Kwon, S.S., Jo, G., Song, S., Kim, S.M., Ko, H.J., Park, S.J., Welland, M.E. and Lee, T. (2008a) Nano Lett. 8 950.
Hong, W.K., Kim, B.J., Kim, T.W., Jo, G., Song, S., Kwon, S.S., Yoon, A., Stach, E.A. and Lee, T. (2008b) Colloids and Surfaces A 313 378.
Hopfield, J.J. (1958) Phys. Rev. 112 1555.
Hopfield, J.J. (1960) J. Phys. Chem. Solids 15 97.
Hopfield, J.J. and Thomas, D.G. (1960) J. Phys. Chem. Solids 12 276.
Hopfield, J.J. and Thomas, D.G. (1963) Phys. Rev. 132 563.
Hopfield, J.J. and Thomas, D.G. (1965) Phys. Rev. Lett. 15 22.
Hutson, A.R. (1960) Phys. Rev. Lett. 4 505.
Kamat, P.V. (2007) J. Phys. Chem. C 111 2834.
Kang, B.S., Heo, Y.W., Tien, L.C., Norton D.P., Ren, F., Gila, B.P. and Pearton, S.J. (2005) Appl. Phys. A 80 1029.
Karuppuchamy, S. and Jeong, J.M. (2005) 93 251.
Kashireninov, O.E., Manelis, G.B. and Repka, L.F. (1982) Russ. J. Phys. Chem. 56 630.
Kent, W. (1958) Philosophy of Science 25 185.
Kim, S.K., Jeong, S.Y. and Cho, C.R. (2003a) Appl. Phys. Lett. 82 562.
Kim, S.W., Kotani, T., Ueda, M., Fujita, S. and Fujita, S. (2003b) Applied Physics Letters 83 3593.
Kirkham, M., Wang, X.D., Wang, Z.L. and Snyder, R.L. (2007) Nanotechnology 18 365304.
Klingshirn, C. (1975) Phys. Stat. Sol. (b) 71 547.
Klingshirn, C. and Haug, H. (1981) Physics Reports 70 315.
Klingshirn, C. (1997) *Semiconductor Optics*, Springer-Verlag, Berlin and Heidelberg.
Klingshirn, C. (2005) Superlatt. Microstruc. 38 209.
Klingshirn, C. (2007) Phys. Stat. Sol. (b) 244 3027.
Ko, H.J., Chen, Y.F., Yao, T., Miyajima, K., Yamamoto, A. and Goto, T. (2000) Appl. Phys.Lett. 77 537.
Koenenkamp, R., Word, R.C. and Schlegel, C. (2004) Appl. Phys. Lett. 85 6004.
Kong, X.Y. and Wang, Z.L. (2004a) Appl. Phys. Lett. 84 975.
Kong, X.Y., Ding, Y., Yang, R.S. and Wang, Z.L. (2004b) Science 303 1348.
Kulkarni, A.J., Zhou, M., Sarasamak, K. and Limpijumnong, S. (2006) Phys. Rev. Lett. 97 105502.
Kumar, N., Dorfman, A. and Hahm, J.I. (2006) Nanotechnology 17 2875.
Kumar, S., Kim, G.-H., Sreenivas, K. and Tandon, R.P. (2007) J. Phys.: Condens. Matter 19 472202.
Lagois, J. (1977) Phys. Rev. B 16, 1699.
Lander, J.J. (1960) J. Phys. Chem. Solids 15 324.
Lany, S., Osorio-Guillen, J. and Zunger, A. (2007) Phys. Rev. B 75 241203.
Laudise, R.A.and Ballman, A.A. (1960) J. Phys. Chem. 64 688.
Law, M., Greene, L.E., Johnson, J.C., Saykally, R. and Yang, P.D. (2005) Nature Mater. 4 455.
Lee, C.J., Lee, T.J., Lyu, S.C., Zhang, Y., Ruh, H. and Lee, H.J. (2006) Appl. Phys. Lett. 81 3648.
Leiter, F., Alves, H., Pfisterer, D., Romanov, N.G., Hofmann, D.M. and Meyer, B.K. (2003)

340 201.
Li, Y., Cai, W.P., Duan, G.T., Cao, B.Q., Sun, F.Q. and Lu, F. (2005) J. Coll. Interface. Sci. 287 634.
Li, Y.J, Feneberg, M., Reiser, A., Schirra, M., Enchelmaier, R., Ladenburger, A., Langlois, A., Sauer, R. and Thonke, K. (2006) J. Appl. Phys. 99, 054307.
Liao, L., Li, J.C., Wang, D.F., Liu, C., Liu, C.S., Fu Q. and Fan, L.X. (2005) Nanotechnology 16 985.
Libbrecht, K.G. (2005) Rep. Prog. Phys. 68 855.
Libbrecht, K.G. (2008) Physics World 21 19.
Limpijumnong, S., Zhang, S. B., Wei, S.-H. and Park, C. H. (2004) Phys. Rev. Lett. 92 155504.
Liu, M.J. and Kim, H.K. (2004) Appl. Phys. Lett. 84 173.
Liu, Y., Dong, J., Hesketh, P.J. and Liu, M.L. (2005) J. Mater. Chem. 15 2316.
Look, D.C., Reynolds, D.C., Sizelove, J.R., Jones, R.L., Litton, C.W., Cantwell, G. and Hrach, W.C. (1998) Solid State Commun. 105 399.
Look, D.C. (2001) Mat. Sci Eng. B 80 383.
Look, D.C. (2005), Semicond. Sci. Tech. 20 S55.
Look, D.C., Mosbacker, H.L., Strzhemechny, Y.M. and Brillson, L.J. (2005) Superlatt. Microstruc. 38 406.
Lorenz, M., Kaidashev, E.M., Rahm, A., Nobis, Th., Lenzner, J., Wagner, G., Spemann, D., Hochmuth, H. and Grundmann M. (2005) Appl. Phys. Lett. 86 143113.
Lu, J. ., Zhang, Y.Z., Ye, Z.Z., Zhu, L.P., Wang, L., Zhao, B.H. and Liang, Q.L. (2006) Appl. Phys. Lett. 88 222114.
Makino, T., Segawa, Y., Kawasaki, M. and Koinuma, H. (2005) Semicond. Sci. Tech. 20 S78.
Mariano, A.N. and Hanneman, R.E. (1963) J. Appl. Phys. 34, 384.
McGlynn, E., Fryar, J., Henry, M.O., Mosnier, J.-P., Lunney, J.G., O' Mahony, D. and dePosada, E. (2003) Physica B, 340-342 230.
Meyer, B.K., Alves, H., Hofmann, D.M., Kriegseis, W., Forster, D., Bertram, F., Christen, J., Hoffmann, A., Strassburg, M., Dworzak, M., Haboeck, U. and Rodina, A.V. (2004) Phys. Stat. Sol. (b) 241 231.
Minami, T. (2005) Semicond. Sci. Technol. 20 S35.
Monroy, E., Omnes, F. and Calle, F. (2003) Semicond. Sci. Technol. 18 R33.
Mosnier, J.-P., O'Haire, R., Boyle, M.A.G., McGuigan, K.G., McGlynn, E. and Henry, M.O. (2006) 4th International Workshop on ZnO and Related Materials, October 3rd – 6th 2006, University of Giessen, Giessen, Germany.
Nobis, T., Kaidashev, E.M., Rahm, A., Lorenz, M. and Grundmann, M. (2004) Phys. Rev. Lett. 93 103903.
O'Haire, R., Meaney, A., McGlynn, E., Henry, M.O., Duclère, J.-R. and Mosnier, J.-P. (2006) Superlattices and Microstructures, 39 153.
Ozgur, O., Alivov, Y.I., Liu, C., Teke, A., Reshchikov, M.A., Dogan, S., Avrutin, V., Cho, S.-J. and Morkoc, H. (2005) J. Appl. Phys. 98 041301.
Pan, Z.W., Dai, Z.R. and Wang, Z.L. (2001) Science 291 1947.
Park, Y.S., Litton, C.W., Collins, T.C. and Reynolds, D.C. (1966) Phys. Rev. 143 512.
Park, Y.S. and Reynolds, D.C. (1967) J. Appl. Phys. 38 756.
Park, W.I., Kim, D.H., Jung, S.W. and Yi, G.C. (2002a) Appl. Phys. Lett. 80 4232.

Park, W.I., Yi, G.C., Kim M.Y. and Pennycook, S.J. (2002b) Adv. Mater. 14 1841.
Park, W.I., Yi, G.C., Kim, M. and Pennycook, S.J. (2003) Adv. Mater. 15 526.
Park, W.I. and Yi, G.C. (2004) Adv. Mater. 16 87.
Park, J.-H., Choi, Y.-J. and Park, J.-G. (2005) J. Crys. Growth 280 161.
Park, N.K., Han, G.B., Lee, J.D., Ryu, S.O., Lee, T.J., Chang, W.C. and Chang, C.H. (2006) Curr. Appl. Phys. 6S1 e176.
Pedley, J.B. and Marshall, E.M. (1983) J. Phys. Chem. Ref. Data 12 967.
Pekar, S.I. (1958) J. Phys. Chem. Solids 5 11.
Phillips, J.C. (1970) Rev. Mod. Phys. 42 317.
Pimpinelli, A. and Villain, J. (1998) *Physics of Crystal Growth*, Cambridge University Press, Cambridge, UK.
Postels, B., Kreye, M., Wehmann, H.-H., Bakin, A., Boukos, N., Travlos, A. and Waag, A. (2007) Superlatt. Microstruc. 42 425.
Qin, Y., Wang, X.D. and Wang, Z.L. (2008) Nature 451 809.
Rajendra Kumar, R.T., Grabowska, J., Mosnier, J.-P., Henry, M.O. and McGlynn, E. (2007a) Superlatt. Microstruc. 42 337.
Rajendra Kumar, R.T., McGlynn, E., McLoughlin, C., Chakrabarti, S., Smith, R.C., Carey, J.D., Mosnier, J.-P. and Henry, M.O. (2007b) Nanotechnology 18 215704.
Recio, J.M., Blanco, M.A., Luaña, V., Pandey, R., Gerward, L. and Staun Olsen, J. (1998) Phys. Rev. B 58 8949.
Reimer, L. (1997) *Transmission Electron Microscopy: Physics of Image Formation and Microanalysis* (4^{th} Ed.), Springer-Verlag, Berlin and Heidelberg.
Reiser, A., Ladenburger, A., Prinz, G.M., Schirra, M., Feneberg, M., Langlois, A., Enchelmaier, R., Li, Y., Sauer, R. and Thonke, K. (2007) J. Appl. Phys. 101 054319.
Reynolds, D.C., Look, D.C., Jogai, B., Litton, C.W., Cantwell, G. and Harsch, W.C. (1999) Phys. Rev. B 60 2340.
Rogers, D.J., Teherani, F.H., Yasan, A., Minder, K., Kung, P. and Razeghi, M. (2006) Appl. Phys. Lett. 88 141918.
Rössler, U. (1999) *Landolt-Börnstein Numerical Data and Functional Relationships in Science and Technology, Semiconductors B: II-VI and I-VII Compounds*, Springer-Verlag, Berlin and Heidelberg (on CD-ROM).
Rowe, J.E., Cardona, M. and Pollak, F.H. (1968) Solid State Comm. 6 239.
Saunders, R. (2008) Private communication of work in progress.
Savikhin, S.F. and Freiberg, A. (1993) J. Lumin. 55 1.
Scharowsky, E. (1953) Zeit. f. Physik 135 318.
Schildknecht, A., Sauer, R. and Thonke, K. (2003) Physica B 340-342 205.
Schmidt, O., Geis, A., Kiesel, P., Van de Walle, C.G., Johnson, N.M., Bakin, A., Waag, A. and Dohler, G.H. (2006) Superlatt. Microstruc. 39 8.
Schmidt, R., Rheinlander, B., Schubert, M., Spemann, D., Butz, T., Lenzner, J., Kaidashev, E.M., Lorenz, M., Rahm, A., Semmelhack, H.C. and Grundmann, M. (2003) Appl. Phys. Lett. 82 2260.
Schrey, H. and Klingshirn, C. (1978) Phys. Stat. Sol. (b) 90 67.
Scott, J.F. (1970) Phys. Rev. B 2 1209.
Shalish, I., Temkin, H. and Narayanamurti, V. (2004) Phys. Rev. B 69 245401.
Shindo, K., Morita, A. and Kamimura, H. (1965) J. Phys. Soc. Jpn. 20 2054.

Silva, S.R.P., Carey, J.D., Guo, X., Tsang, W.M. and Poa, C.H.P. (2005) Thin Solid Films 482 79.
Smith, D.L. (1995) *Thin Film Deposition: Principles and Practice*, McGraw-Hill, USA.
Song, J. H., Wang, X. D., Riedo, E. and Wang, Z. L. (2005) J. Phys. Chem. B 109 9869.
Tasker, P.W. (1979) J. Phys. C: Solid State Phys. 12 4977.
Thomas, D.G. (1960) J. Phys. Chem. Solids 15 86.
Tien, L.C., Norton, D.P., Pearton, S.J., Wang, H.T. and Ren, F. (2007) Appl. Surf. Sci. 253 4620.
Tobin, G., McGlynn, E., Henry, M.O., Mosnier, J.P., de Posada, E. and Lunney, J.G. (2006) Appl. Phys. Lett. 88 071919.
Tomzig E. and Helbig, R. (1976) J.Lumin. 14 403.
Travnikov, V.V., Freiberg, A. and Savikhin, S.F. (1990) J. Lumin. 47 107.
Tsukazaki, A., Ohtomo, A., Onuma, T., Ohtani, M., Makino, T., Sumiya, M., Ohtani, K., Chichibu, S.F., Fuke, S., Segawa, Y., Ohno, H., Koinuma, H. and Kawasaki, M. (2005) Nature Mat. 4 42.
Tusche, C., Meyerheim, H.L. and Kirschner, J. (2007) Phys. Rev. Lett. 99 026102.
Van de Walle, C.G. (2001) Physica B 308-310 899.
Van de Walle, C.G. (2006) Physica B 376 1.
Vanheusden, K., Warren, W.L., Seager, C.H., Tallant, D.R., Voight, J.A. and Gnade, B.E. (1996) J. Appl. Phys. 79 7983.
van Vugt, L.K., Ruhle, S., Ravindran, P., Gerritsen, H.C., Kuipers, L. and Vanmaekelbergh, D. (2006) Phys. Rev. Lett. 97 147401.
Voss, T., Bekeny, C., Wischmeier, L., Gafsi, H., Boerner, S., Schade, W., Mofor, A.C., Bakin, A. and Waag, A. (2006) Appl. Phys. Lett. 89 182107.
Wang, Z.L., Kong, X.Y. and Zuo, J. M. (2003) Phys. Rev. Lett. 91 185502.
Wang, Z.L. (2004) J. Phys.: Condens. Matter 16 R829.
Wang, H.T., Kang, B.S., Ren, F., Tien, L.C., Sadik, P.W., Norton, D.P., Pearton, S.J. and Lin, J.S. (2005) Appl. Phys. Lett. 86 243503.
Wang, X.D., Song, J.H. and Wang, Z.L. (2006a) Chem. Phys. Lett. 424 86.
Wang, W.Z., Zeng, B.Q., Yang, J., Poudel, B., Huang, J.Y., Naughton, M.J. and Ren, Z.F. (2006b) Adv. Mater. 18 3275.
Wang, Z.L. (2007) Materials Today 10 20.
Wang, Z.L. (2008) J. Nanosci. Nanotech. 8 27.
Weber, L. (1923) Zeitschrift für Kristollographie 58 398.
Wei, M., Zhi, D. and MacManus-Driscoll, J.L. (2005) Nanotechnology 16 1364.
Willander, M., Zhao, Q.X., Hu, Q.-H., Klason, P., Kuzmin, V., Al-Hilli, S.M., Nur, O. and Lozovik, Y.E. (2008a) Superlatt. Microstruc. 43 352.
Willander, M., Wadeasa, A., Klason, P., Yang, L., Lubana Beegum, S., Raja, S., Zhao, Q. X. and Nur, O. (2008b) Proc. SPIE 6895 68950O.
Wischmeier, L., Voss, T., Ruckmann, I., Gutowski, J., Mofor, A.C., Bakin, A. and Waag, A. (2006a) Phys. Rev. B 74 195333.
Wischmeier, L., Voss, T., Boerner, S. And Schade, W. (2006b) Appl. Phys. A 84 111.
Woll, C. (2007) Prog. Surf. Sci. 82 55.
Xu, C.X., Sun, X.W., Dong, Z.L., Yu, M.B., My, T.D., Zhang, X.H., Chua, S.J. and White, T.J. (2004) Nanotechnology 15 839.

Xu, F., Yu, K., Li, G.D., Li, Q. and Zhu, Z.Q. (2006) Nanotechnology 17 2855.
Yan, Y.F., Li, J.B., Wei, S.-H. and Al-Jassim, M.M. (2007) Phys. Rev. Lett. 98 135506.
Yang, P., Yan, H., Mao, S., Russo, R., Johnson, J., Saykally, R., Morris, N., Pham, J., He, R. and Choi, H.-J. (2002) Adv. Func. Mater. 12 323.
Yang, Y.H., Wang, B., Xu, N.S. and Yang, G.W. (2006) Appl. Phys. Lett. 89 043108.
Zamfirescu, M., Kavokin, A., Gil, B., Malpuech, G. and Kaliteevski, M. (2002) Phys. Rev. B 65 161205.
Zhang, S.B., Wei, S.-H. and Yan, Y.F. (2001) Physica B 302-303 135.
Zhao, D., Andreazza, C., Andreazza, P., Ma, J., Liu, Y. and Shen, D. (2004) Chem. Phys. Lett. 399 522.
Zu, P., Tang, Z.K., Wong, G.K.L., Kawasaki, M., Ohtomo, A., Koinuma, H. and Segawa, Y. (1997) Solid State Commun. 103 459.